ENGINEERING RESEARCH INSTITUTE
UNIVERSITY OF MICHIGAN
ANN ARBOR

Interim Technical Report No. 4

PRESSURE DROP AND FLOW PATTERNS IN THE IMPINGEMENT SECTION OF AN OIL-BATH AIR CLEANER

Seymour Calvert
Henry J. Hartog
Hadley J. Smith
Robert M. Pease
J. Louis York

Project 2233

DETROIT ARSENAL, U. S. ARMY
CONTRACT NO. DA-20-089-ORD-36962
CENTER LINE, MICHIGAN

May 1955

TABLE OF CONTENTS

ABSTRACT

This report summarizes the progress to date on the study of the impingement section of the oil-bath-type air cleaner. This work comprises one aspect of the overall engineering investigation into the performance of induction air cleaners and their principles of operation. As stated in the contract for this work, the objectives of the investigation are as follows:

"a. Determine the basic principles involved in the mechanism of operation of existing air cleaners and measure the limits and quantitative effect of these principles on performance with first emphasis upon the oil bath units now employed extensively.

"b. Organize these principles and quantitative measurements to furnish a basis for evaluating new designs, developing improvements in existing air cleaners, and developing new designs.

"c. Furnish technical background for preparation of revised specifications for air cleaners."

The method of procedure was also concisely described in the contract as being in accordance with the following (along with other points):

"b. The Contractor shall conduct experimental studies on cleaners to determine flow patterns, comparative performance of individual components of different design and construction material, and effect of varying operating conditions. These will include photographic studies of performance, measurement of pressure loss, dust removal, and oil losses."

The investigation has proceeded along the general lines given above and has thus far been concerned with oil-bath-type air cleaners only. Oil-bath cleaners as presently designed are typified by incorporating an impingement section and a "packed section" following it. In the impingement section, the incoming (dusty) air impinges upon an oil-wetted baffle plate or cup and is turned and directed upward into the packed section. The packed section is usually annular in cross section and is filled with fibrous packing, such as wire screen. Both sections serve to separate dust from the air, although the dust collection efficiency of the impingement section is of little significance since the packed section has a higher efficiency which

is not increased by the addition of the impingement section efficiency.

Consequently, our main interest in the impingement section centers around its effect on the flow of air. It functions incidentally to provide a flow of oil into the packed section and to establish a tranquil zone in which collected dust can settle out of the oil. The two main questions whose study is reported here are:

1. What is the relationship between pressure drop, air flow rate, impingement section geometry, and oil flow rate?

2. What are the flow patterns in the impingement section and in the air stream just entering the packed section?

Chapters I and II deal with the first question. Experimental work on the flow of air through various models of impingement section geometry is described in Chapter I. Analyses of the data gave an empirical relationship between pressure drop, air flow rate, and geometric parameters such as tube and baffle sizes and the distance between the tube outlet and the baffle.

This relationship is valid over a wide range of geometric parameters and provides a convenient method for prediction of pressure drop for air flow through baffled systems such as the impingement section. The data on two-phase flow (air and oil) showed that at high flow rates the behavior of the two-phase system can be described by the single-phase relationships with accuracy which is adequate for design purposes.

An analysis of the problem of air flow through baffled systems of this type is given in Chapter II. The result of the analysis is a generalized method, based on ideal fluid-flow theory, which predicts pressure drop versus flow rate relationships which agree satisfactorily with both the data on experimental impingement-section models and the data on a production-model Donaldson Company air cleaner. Experimental data on the pressure drop versus flow relationship for a production-model Donaldson Company 410-cfm air cleaner are also presented and analyzed in this chapter. Possible design modifications are indicated which would alleviate the undesirable conditions of high pressure drop in the entry section and uneven flow distribution in the outlet section of this cleaner.

Flow visualization experiments on impingement section models are described in Chapter III. The principal methods of determining the flow patterns involved visual observation and were a smoke-stream technique used on a three-dimensional model and a free-surface water-tunnel technique used on a two-dimension model. Photographs and drawings of these experiments show the flow patterns encountered. Design modifications are suggested for attaining more desirable flow characteristics. The velocity distribution in the stream entering the packed section is uniform in almost all (geometric) cases.

CHAPTER I

EXPERIMENTAL STUDIES OF THE PRESSURE DROP ACROSS THE AIR-CLEANER BAFFLE CUP AND AN EMPIRICAL CORRELATION OF THE DATA

Introduction

The study of the fluid-flow characteristics in the impingement section of an oil-bath air cleaner required the experimental determination of the flow data. Several types of experimental models representing impingement-section geometry were designed and built in order to permit the study of various geometric and size combinations. The apparatus in the form of its final modification is described here.

This chapter covers the description of the experimental apparatus and procedure, the data, and an empirical correlation of the data. Some specific data are given for two-phase (air and oil) flow, but this system was not studied extensively since it was found that at the higher air flow rates the pressure drop for single-phase flow is approximately the same as for two-phase flow.

Apparatus

The experimental setup used to obtain the pressure-drop data discussed in this report is reproduced schematically in Fig. 1.

The air-cleaner model consisted of an outer shell or housing (A), a vertical center tube (B), and a baffle cup (C). Means were provided for varying the geometry by installing center tubes of different diameters, using baffle cups of varying heights and diameters and adjusting the baffle spacing (H).

The airstream was brought into the model through the center tube, was deflected upward by the baffle and then discharged into the room through the exit orifice (L).

The rate of flow was controlled by the adjustable valve (E) and was measured on a Floguide rotameter installed upstream of the model at (F). During two-phase-flow operation SAE No. 10 oil was circulated through the cleaner by a centrifugal pump (G). The oil flow rate was read on the oil flowmeter (I).

The static pressure taps were placed at stations (1) and (3), as shown, where photographs of the streamlines indicated that the main stream was parallel to the walls. It will be shown later that the pressure difference between these stations does not differ from the drop across the baffle.

The pressure readings were taken on the differential manometer (J) and the pressure upstream of the air rotameter was read on manometer (K).

Additional experiments were made on jets impinging on flat plates. These tests were conducted with essentially the same setup while the model was open to the atmosphere.

Experimental Work

The testing procedure followed was aimed at determining the pressure drop ΔP across the baffle in terms of the following parameters:

1. Rate of airflow Q
2. Center-tube diameter d
3. Baffle-cup diameter D
4. Baffle-cup height H
5. Baffle spacing h
6. Rate of oil flow W

A first series of runs was concerned with comparing the results for one- and two-phase flows. The air flow rate was varied between zero and 6000 scfh and the tests were repeated for several baffle spacings. The oil flow rate was varied from zero to 4 lb/min.

It was established during these runs that, while a correlation of the data obtained for two-phase flow would be extremely complicated, the results at higher airstream velocities comparable to those occurring in the air cleaner could be represented with sufficient accuracy by the data obtained for one-phase flow. Therefore, it was decided to discontinue two-phase runs and concentrate on determining the pressure loss in terms of the remaining air flow and geometry parameters.

The range of parameters tested was as follows:

d:	from 1.00"	to 2.25"
D:	from 3.00"	to 6.00" and ∞
H:	from 0	to 2.50"
h:	from 0.125"	to 2.625"
Q:	from 0	to 100 scfm

The combination of air flows and center-tube diameters used corresponded to Reynolds' numbers in the center tube ranging from 6,000 to 162,000.

Results

1. GENERAL ASPECT OF THE FLOW; ASSUMPTIONS THAT CAN BE DERIVED

A study of the streamlines through the model has shown that at the baffle-cup exit the main stream is surrounded by two eddies, one forming between the flow and the center tube, the other between the flow and the external wall of the cleaner. The horizontal pressure differential across these eddies is equal to zero. This has been substantiated by static pressure traverses (see Fig. 2) yielding a constant pressure distribution.

The static pressure at cup level in the main flow varies slightly in the horizontal direction, reaching a minimum at about the middle of the airstream. The difference between average and maximum pressure in the stream is about 10 percent. This difference has not been taken into account in the presentation of data as it affects all readings and does not alter appreciably the shape of the curves obtained. A corrective factor will be introduced later to compensate for this effect. The pressure above cup level, on the other hand, is constant and equals the pressure in the eddies at the same elevation.

The flow pictures taken indicate that in the neighborhood of stations (1), (2), and (3) the average velocities of the airstream were confined to the vertical direction, having negligible horizontal components or none. This simplifies the relations between the flow parameters in the regions around the three stations by reducing the analysis to that applicable in the case of one-dimensional flow.

An additional assumption can be introduced, qualifying the flow as incompressible. The error entailed is relatively small at low velocities and will not be considered here.

Under these conditions it can be shown that the actual pressure drop across the baffle ΔP, which is equal to the pressure difference between stations (1) and (2), does not differ from the drop measured between stations (1) and (3), except for the correction mentioned previously.

Referring to Fig. 3, an expression stating conservation of momentum can be written for the flow through the cylindrical-washer-shaped control surface as shown. This expression is:

$$A(p_2 - p_3) = \rho Q(V_3 - V_2)$$

where

A = annular area between center tube and outer wall,
p_2, p_3 = static pressures at (2) and (3),
V_2, V_3 = average velocities at (2) and (3), and
ρ = density of air.

Rearranging:

$$p_2 - p_3 = \frac{\rho Q}{A}(V_3 - V_2).$$

The minimum value of area A during the experiments was: $A = 0.82$ ft^2.

The density of air under standard conditions can be taken as: $\rho = 238 \times 10^{-5}$ slugs/ft^3.

Using exaggerated values of the flow parameters,

$$Q = 7200 \text{ scfh}$$
$$|V_3 - V_1| = 50 \text{ ft/sec},$$

we obtain:

$$|p_2 - p_3| = .05 \text{ inch } H_2O.$$

This value, although exaggerated, is smaller than the sensitivity limit of the manometer used and can safely be neglected. Therefore:

$$\Delta P = p_1 - p_2 = p_1 - p_3 .$$

The data plotted on Fig. 3 verifies this result by showing that static pressures at cup level and 1-1/2 inches above cup level are the same.

2. TWO-PHASE FLOW

A representative cross section of the data obtained for two-phase flow has been condensed in Fig. 4. It indicates that at high air flows the pressure drop varies approximately as the square of the air flow rate. A comparison with Fig. 5 will show that under these conditions it approaches very closely the drop obtained during dry testing.

At low velocities there is a pronounced increase over one-phase flow results, then a recession occurs in the curves. This recession is due to the cupping effect of the oil contained in the baffle. The original high pressure difference is due to the head of oil in the cup. As velocities are progressively increased, part of the oil is blown out of the cup and its surface is forced into a smooth concave shape. This decreases the pressure loss which reaches a minimum when all the oil is blown out. If the velocities are further increased, only a thin film of oil remains in the bottom of the cup and the pressures vary like those obtained in the dry runs.

The effect on the curves of increased baffle spacings is to retard their recovery.

3. ONE-PHASE FLOW

Figure 5 has been included in order to provide a basis for comparison between dry and two-phase operation under the same conditions. The curves corresponding to other values of the remaining parameters exhibit the same general shape and compare in the same way to corresponding wet runs.

Correlation of the Data for One-Phase Flow

1. PREDICTED GENERAL FORM OF THE RELATION

In attempting a correlation of the experimental results it will be helpful to consider the following facts:

The physical state of a fluid is described by its pressure, density, and temperature. Its dynamic characteristics are described by its velocity, density, and viscosity and by the geometry of the region in space through

which it flows. If conditions are such that the fluid can be considered as incompressible, its state is determined by its pressure and density alone.

These considerations suggest that the flow can be expected to satisfy a relation of the general form

$$F\left\{\Delta P, V, \rho, \mu, h, D, H, d\right\} = 0 , \tag{1}$$

where the variables are the flow parameters and quantities describing the geometry, namely:

ΔP = pressure difference across the baffle
V = velocity (taken as the average approach velocity in the center tube)
ρ = density
μ = viscosity
h = baffle spacing
D = baffle diameter
H = baffle height
d = center-tube diameter.

This relation is easily reduced by dimensional analysis to a new function of dimensionless variables:

$$F'\left\{\frac{\Delta P}{\rho\frac{V^2}{2}}, \frac{\rho V d}{\mu}, \frac{h}{d}, \frac{D}{d}, \frac{H}{d}\right\} = 0 . \tag{2}$$

Letting

$$K = \frac{\Delta P}{\rho\frac{V^2}{2}} ,$$

$$Re = \frac{\rho V d}{\mu} ,$$

and rewriting the relation explicitly,

$$K = F\left\{Re, \frac{h}{d}, \frac{D}{d}, \frac{H}{d}\right\} . \tag{3}$$

Re is readily recognized as the Reynolds' number in the center tube. K will be identified as the pressure coefficient and is such that

$$\Delta P = K \rho \frac{V^2}{2} \quad . \tag{4}$$

ΔP is determined, therefore, when K and V are known. V, being the average velocity in the center tube, is given by

$$V = \frac{Q}{\frac{\pi d^2}{4}}$$

and (4) can be restated:

$$\Delta P = K \rho \frac{Q^2}{2\left(\frac{\pi d^2}{4}\right)^2} \quad . \tag{5}$$

In either form, ΔP, for any given air flow, will be determined directly by K.

2. EMPIRICAL DETERMINATION OF K

A mathematical analysis of the flow based on the principles of fluid mechanics would be expected to lead to a relation similar to Equations (1), (2), or (3). It is well known, however, that such an analysis has been carried out only for extremely simplified cases of fluid flow. In general, the differential equations describing the motion of the fluid cannot be solved. The derivation of an approximate formula for the pressure drop based on simplifying assumptions is given in another section of this report. Here we shall attempt to bypass the difficulty by relying entirely on the experimental data. The pressure coefficient will be determined graphically by plotting

$$K = \frac{\Delta P}{\rho \frac{Q^2}{2\left(\frac{\pi d^2}{4}\right)^2}}$$

from results obtained in the experiments. Figures 6, 7, 8, and 9 are used

to illustrate the behavior of K in terms of each of the variables. Only typical curves are shown and it should be kept in mind that the shape of the curves is not altered when the constant parameters on each graph are given different numerical values.

A. Effect of the Reynolds' Number.—Figure 6 is a plot of K versus Re. The graph indicates that in the range of Reynolds' numbers above 20,000, K varies little with Re, decreasing slightly as Re increases. The amount by which this variation is affected by the other parameters has not been accurately determined, and on the computation curve given in Fig. 9 K has been considered constant with respect to the Reynolds' number. Values of the pressure coefficient read on this curve will be a few percent too low for Re $< 70{,}000$ and a few percent too high for Re $> 70{,}000$. This point may be further investigated under the present contract.

Values of K for Re under 20,000 are outside the range of normal operation of the air cleaner and will not be discussed here.

B. Effect of h/d.—Figure 7 shows the variation of K with h/d. The pressure coefficient is a decreasing function of the variable depending mainly on $\{h/d\}^{-2}$.

C. Effect of D/d and H/d.—The effect of these two parameters has not been separated. It was apparent, however, that K increased with D/d while it decreased with H/d. The best expression for their combined effect was found to be a relation in the form

$$K = g\left\{\frac{D/d}{(H/d)^{1/2}}\right\} .$$

A few characteristic plots of this function are shown in Fig. 8.

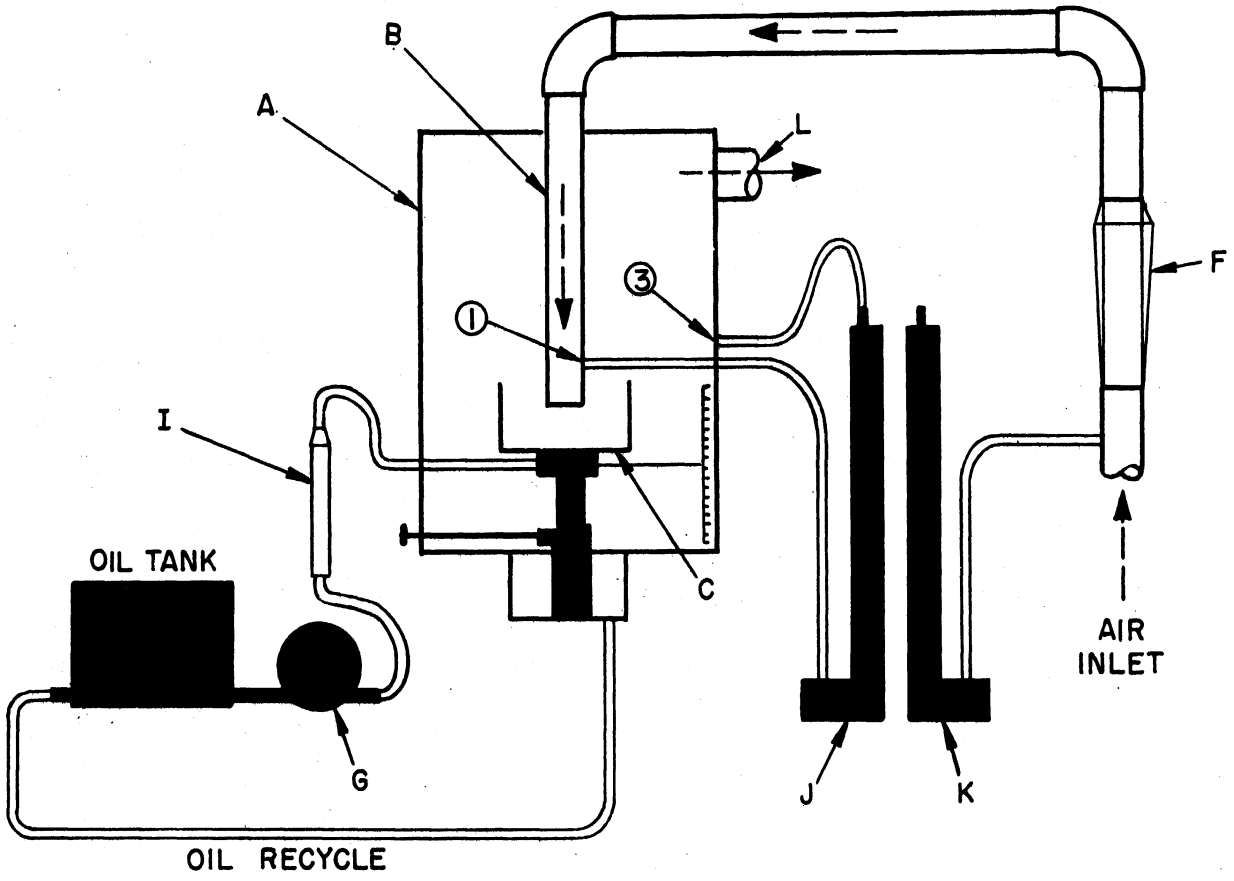

A. HOUSING
B. CENTER TUBE
C. BAFFLE CUP
F. AIR ROTAMETER
G. OIL PUMP
I. OIL ROTAMETER
J&K MANOMETER
L. EXIT ORIFICE

Fig. 1. Impingement section, oil-bath air-cleaner model.

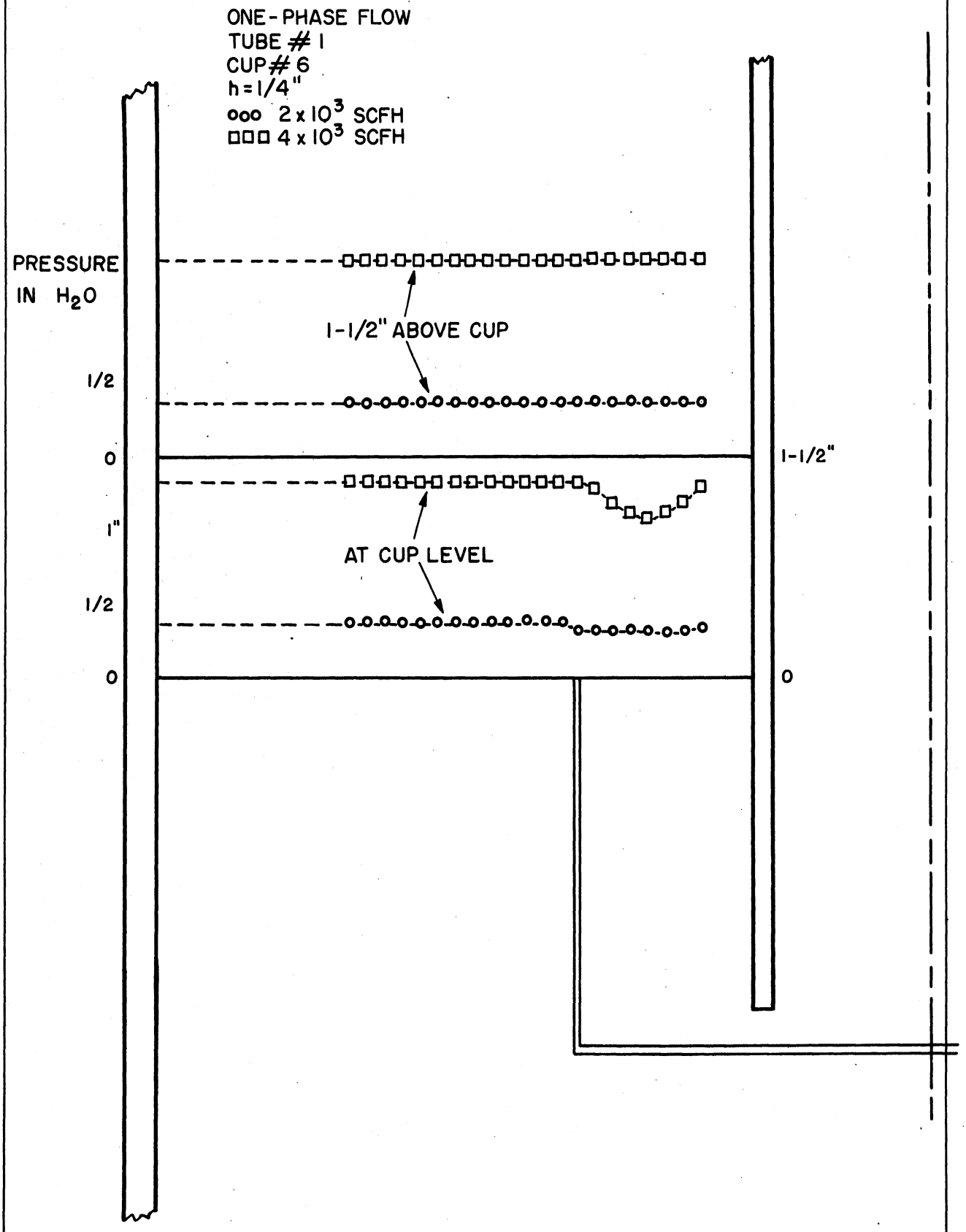

Fig. 2. Air-cleaner tests. Static pressure distribution.

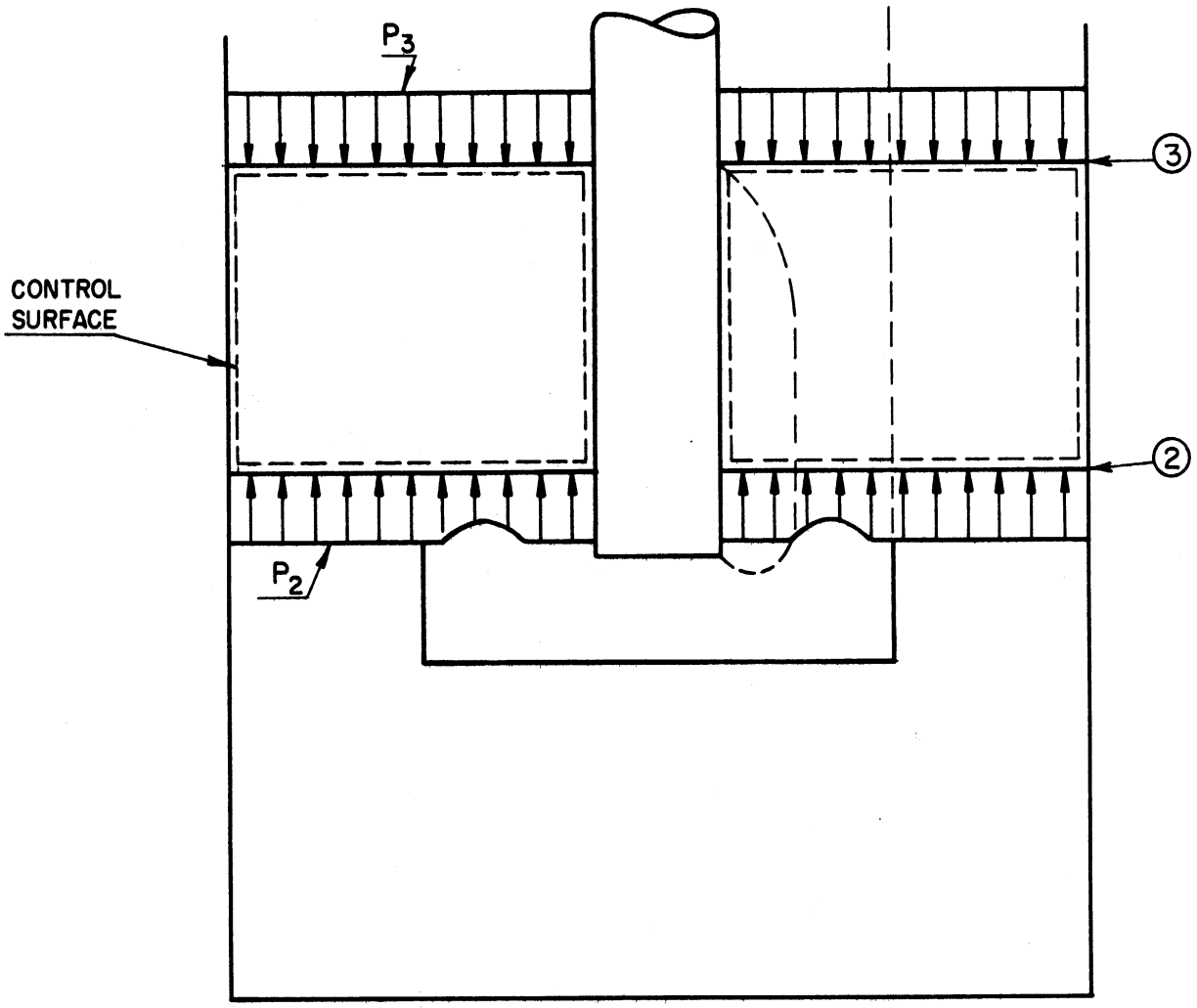

Fig. 3.

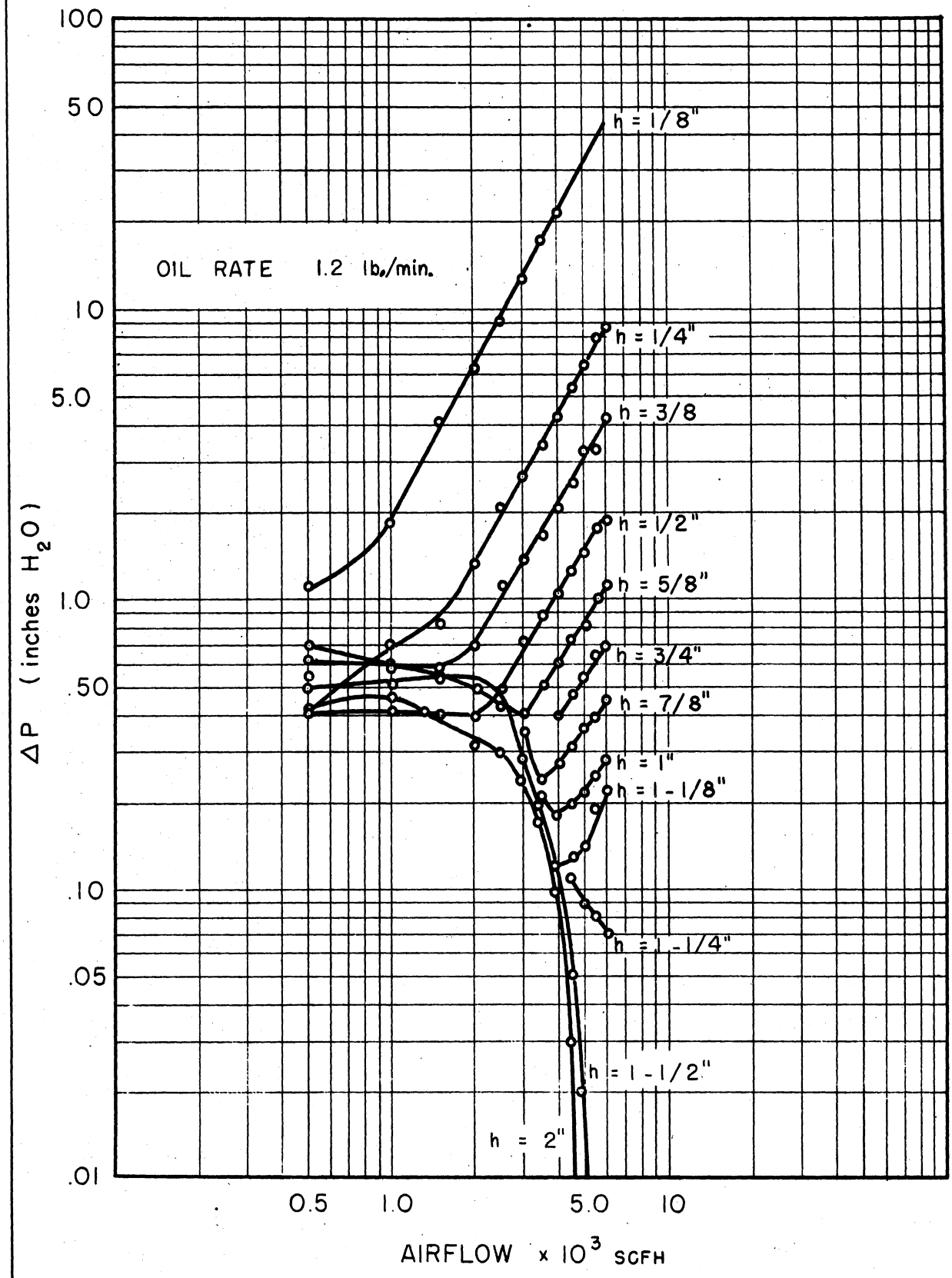

Fig. 4. Air-cleaner tests. Pressure drop vs air flow for two-phase flow.

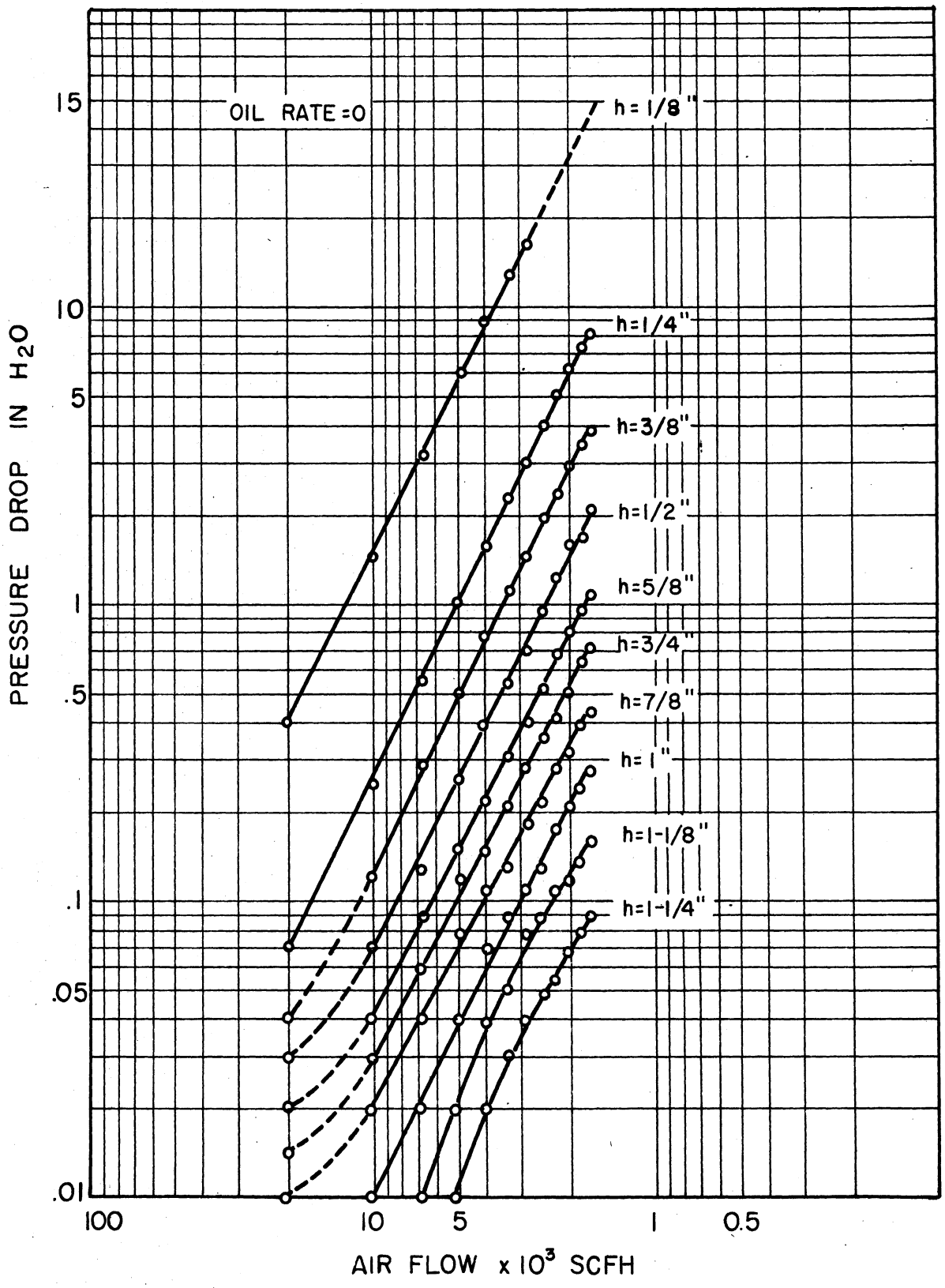

Fig. 5. Air-cleaner tests. Pressure drop vs air flow.

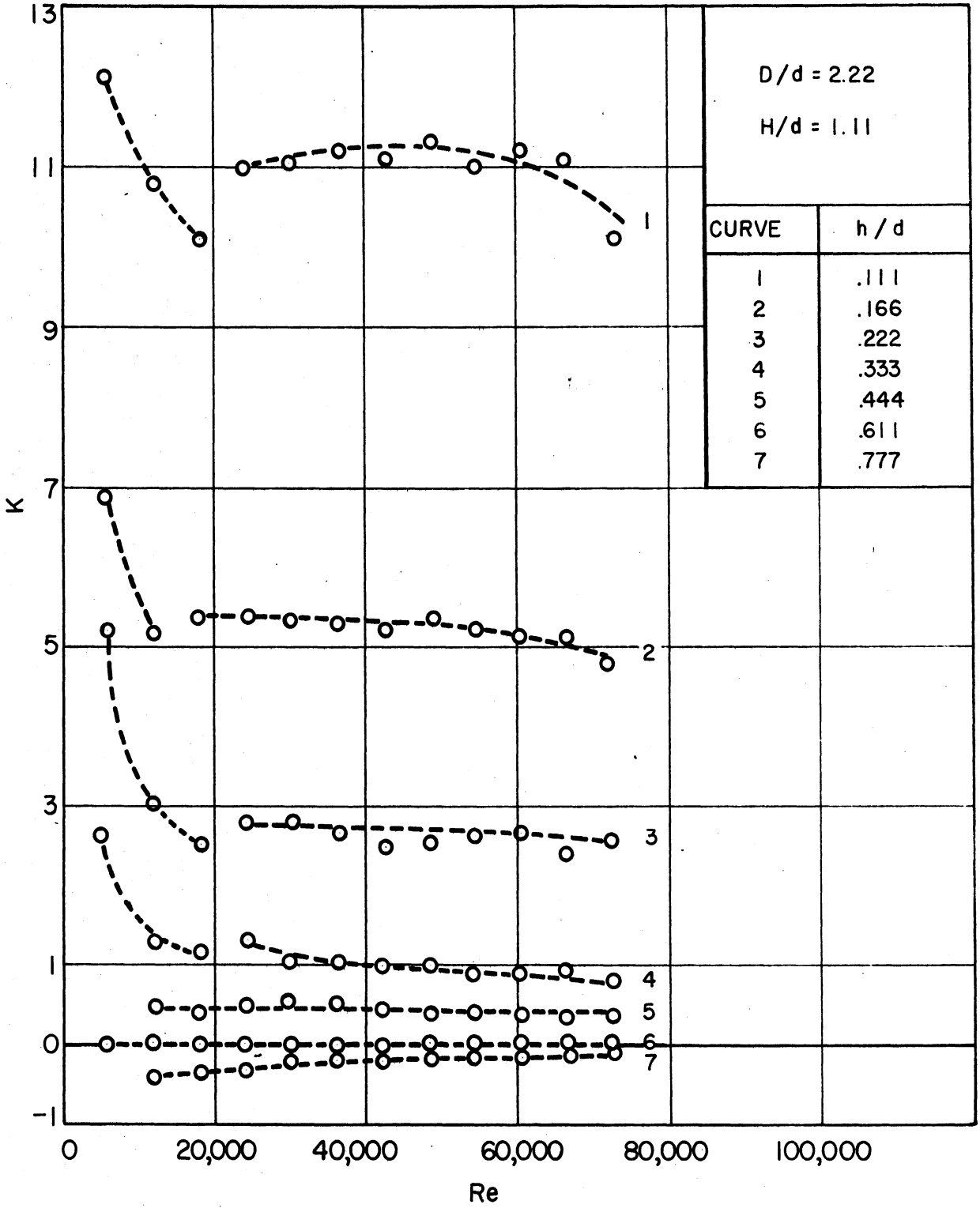

Fig. 6. Air-cleaner tests. Variation of K with Reynolds' number.

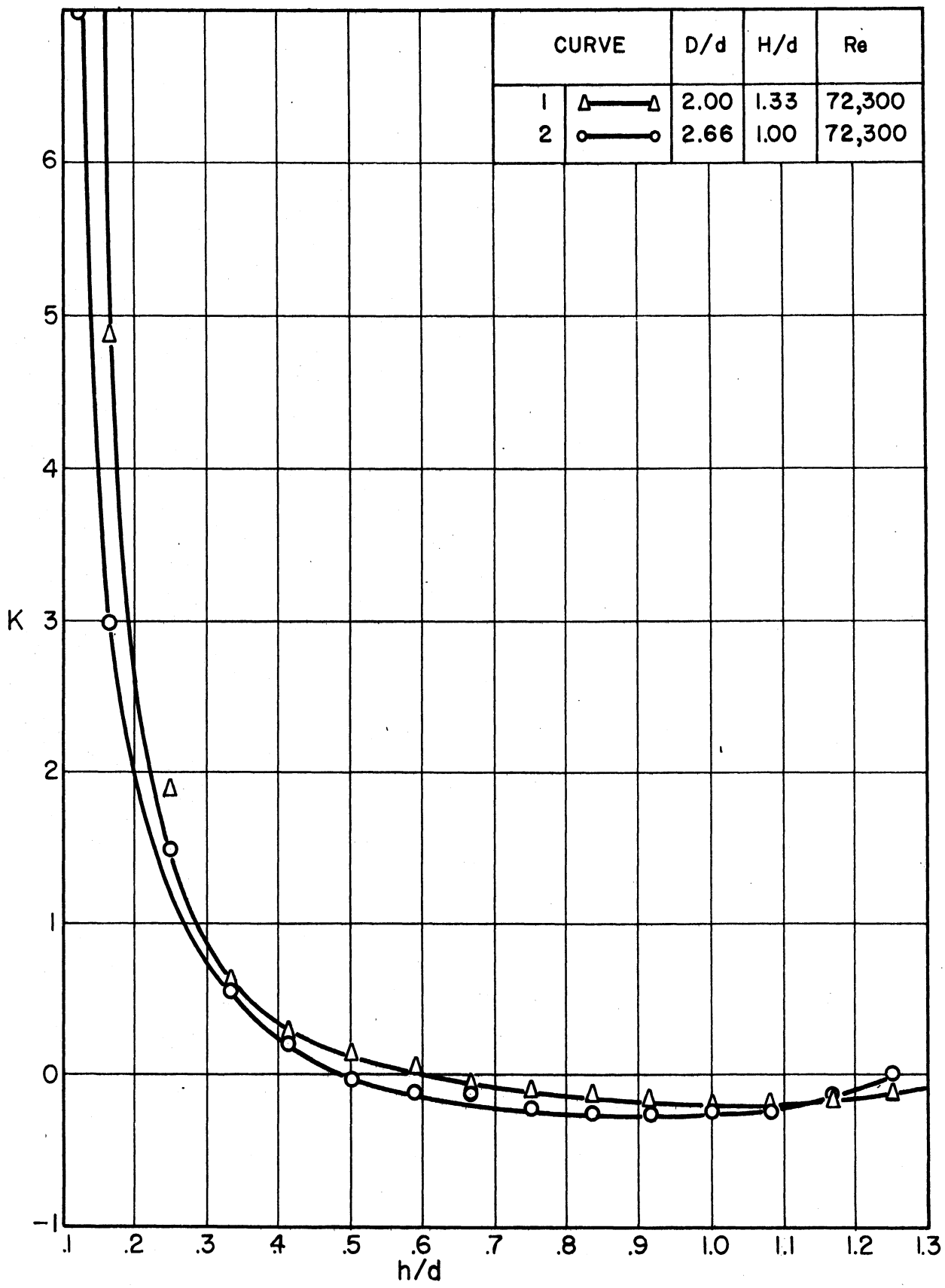

Fig. 7. Air-cleaner tests. Variation of K with h/d.

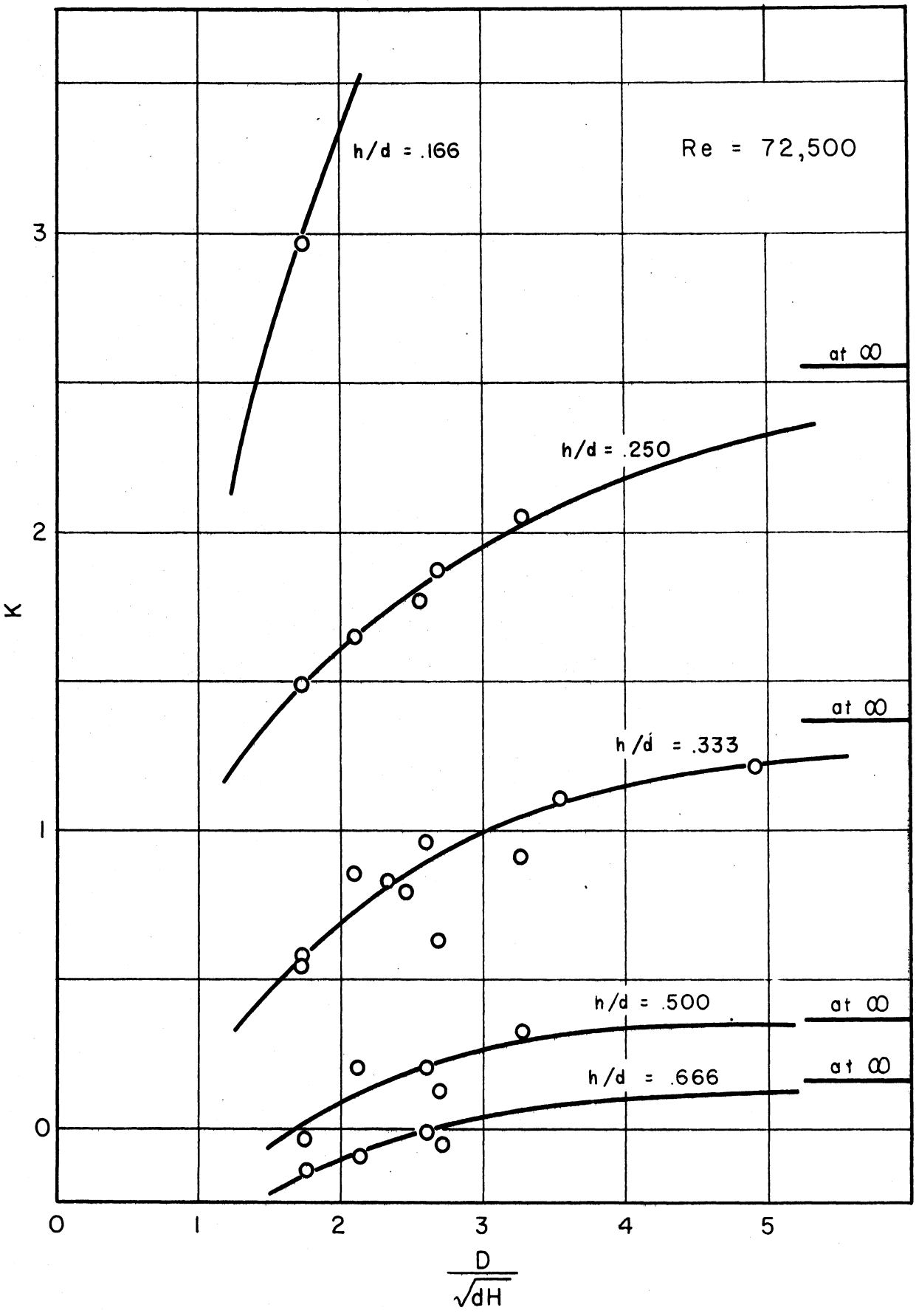

Fig. 8. Air-cleaner tests. K as a function of D/d, H/d.

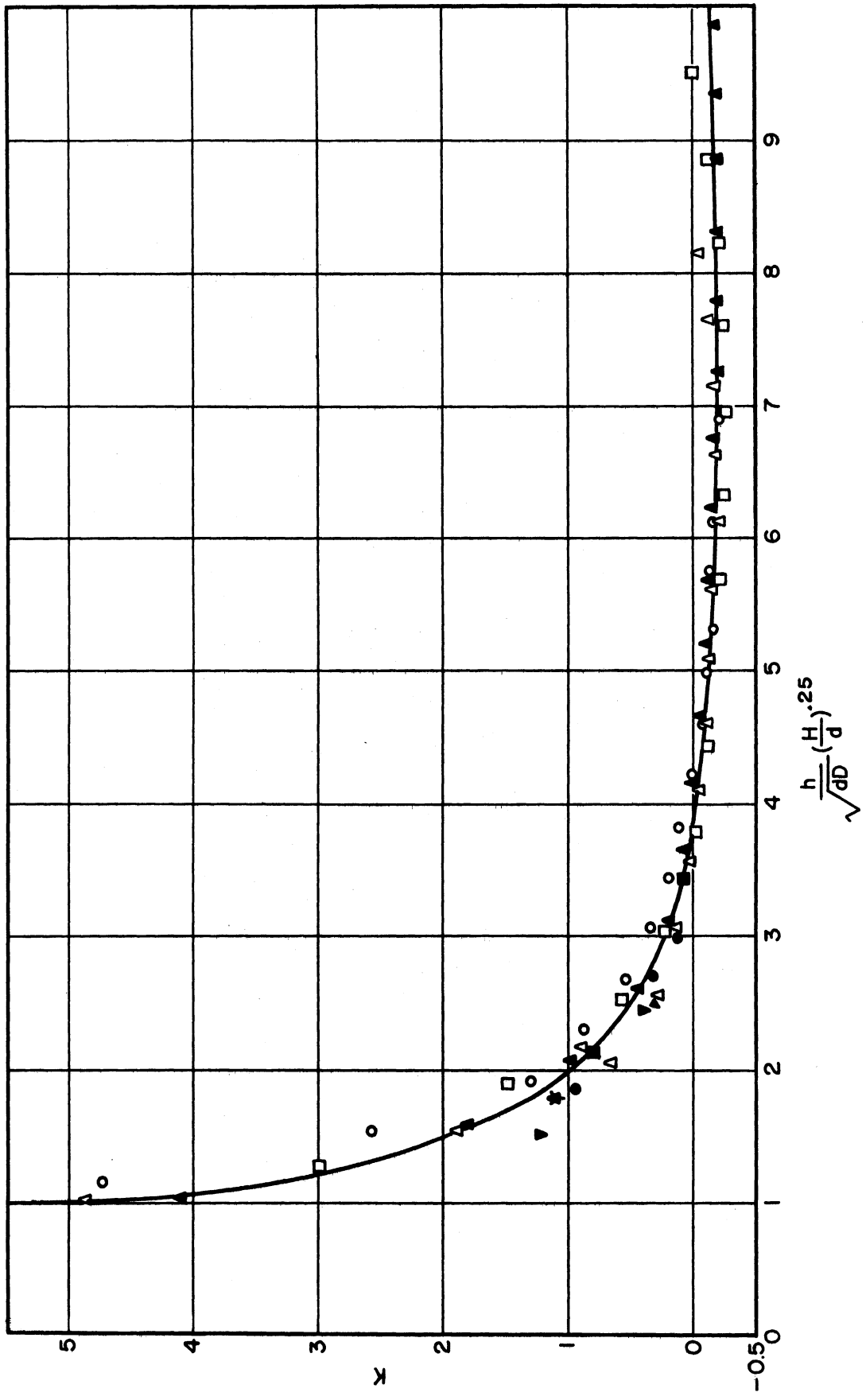

Fig. 9. Air-cleaner tests. K in terms of cleaner geometry.

CHAPTER II

AN ANALYSIS OF PRESSURE DROP AND PRESSURE LOSS IN THE IMPINGEMENT SECTION AND EXPERIMENTAL DATA ON THE CIRCUMFERENTIAL DISTRIBUTION OF AIR FLOW IN AN AIR CLEANER

Introduction

The first several sections of this chapter describe a theoretical analysis and experimental verification of the pressure drop in the cup region of the experimental apparatus (Fig. 10). Following sections discuss a similar study for the baffle region of the Donaldson 410-cfm air cleaner (Fig. 11). Attention is given to an analysis of experimental data concerning the distribution of pressure drop and air flow throughout all the regions of the cleaner. Conclusions are presented in the final section.

The experimental program can be summarized briefly. The pressure drop in the cup region of the test apparatus described in Chapter I was measured, with and without the introduction of oil into the cup, as a function of the rate of air flow and the dimensions of the cup and down-tube. Measurements with and without oil were also made of the pressure drop in the baffle and other regions of the Donaldson cleaner as a function of the air flow rate. In this case, the dimensions of the flow boundaries remained constant.

Discussion of the Variables and Parameters of the Cup-and-Tube Test Apparatus

Figure 10 defines the variables entering into the formula for the pressure drop in the cup region between points 1 and 4. Since conditions at points 2 and 3 are used only temporarily in the development of the formula, the pressure drop proves to be a function of only quantities associated with locations 1 and 4; that is, h, D, d, ρ, and V_1, or

$$\Delta P = f(h, D, d, \rho, V_1) . \qquad (6)$$

It proves possible to express the relationship in the alternative and more instructive form:

$$K = f\left(\frac{h}{d}, \frac{D}{d}\right), \tag{7}$$

where

$$K = \frac{\Delta P}{1/2\ \rho V_1^2} = \text{Pressure drop expressed in "velocity heads."} \tag{8}$$

Theoretically, the dimensionless pressure drop K should also be a function of L and H (Fig. 10) and also of the flow Reynolds' number, R. That is, (7) should be replaced by

$$K = f\left(\frac{h}{d}, \frac{D}{d}, \frac{H}{d}, \frac{L}{d}, R\right) . \tag{9}$$

However, L and H prove experimentally to be negligible factors for the values of the other variables (h, D, d, ρ, and V_1) of interest in the air cleaner problem. We may define the Reynolds' number as

$$R = \frac{V_1 d}{\nu} .$$

Therefore, R increases with V_1 and thus with the volumetric rate of flow Q. At high values of R, the latter may be expected to have little effect on the pressure drop; the experimental data showed this to be true. The higher values of R in the test apparatus correspond to the lower end of the range of R encountered in the engine air cleaner so R may be neglected for the baffle region (see Fig. 11). Thus, it is not surprising that a relation of the type of Equation (7) also proves to be sufficient for the cleaner baffle region.

For purposes of plotting and understanding Equation (7), it is convenient to express K as

$$K = f\left(\frac{A_h}{A_4}, \frac{D}{d}\right) \tag{10}$$

where (A_h/A_4) is the ratio of the cylindrical area for flow under the down tube ($A_h = \pi dh$) to the cross-sectional area of the air stream at point 4 (Fig. 10). As will be seen, K is plotted against (A_h/A_4) with D/d as a parameter.

Experimental Values and Theoretical Relations for the Pressure Drop in the Cup Region of the Test Apparatus

The experimental values of K (the pressure drop in velocity heads) are computed in Table I, using the measured values of the pressure drop and the flow rate. In Fig. 12, K is plotted in terms of the variables of Equation (10).

To determine a theoretical formula for K, we must examine the characteristics of the air flow. The water-channel tests of two-dimensional air cleaner models, described in Chapter III, showed that the air stream and eddies have the general form shown in Fig. 10. Velocity traverses made with a pitot impact tube showed the velocity to be essentially uniform over the cross section at point 4. A uniform velocity distribution may also be assumed to exist at point 2, since it is in the neighborhood of the stagnation point* (point 0), and because the air stream undergoes a rapid contraction as point 2 is approached. A uniform distribution of velocity over the cross section at 1 may be assumed from the water-channel tests of the two-dimensional models of the air cleaner.

The flowing air will be assumed to be incompressible since the maximum pressure drop,

$$\Delta P = p_1 - p_4 , \qquad (10a)$$

in all tests was less than 3 percent of the atmospheric pressure and the resulting error in the calculations which follow is generally less than this amount. Consequently, the Bernoulli energy equation for the flow between points 1 and 4 (Fig. 10) is

$$p_1 + 1/2(\rho V_1^2) = p_4 + 1/2(\rho V_4^2) + p_L = p_4 + 1/2(\rho V_4^2) + C_L\,(1/2\rho V_1^2) \qquad (11)$$

*H. Schlichting, NACA TN No. 1217 (April 1949), p. 34.

where P_L is the pressure loss and C_L is the coefficient of pressure loss due to dissipation of energy, primarily into heat. The volumetric flow is the same at 1 and 4, that is,

$$Q = V_1 A_1 = V_4 A_4 . \tag{12}$$

Then from (11) and (12),

$$p_1 - p_4 = 1/2(\rho V_1^2)\,(1 - V_4^2/V_1^2) + 1/2(C_L \rho V_1^2) , \tag{13}$$

or

$$K = (1 - A_1^2/A_4^2) + C_L . \tag{14}$$

From Fig. 10, $A_1 = (\pi d^2)/4$ and

$$A_4 < (\tfrac{1}{4})\,\pi\,(D^2 - d^2) \tag{15}$$

so that

$$K < \left\{1 - \left[\frac{1}{(\frac{D}{d})^2 - 1}\right]^2\right\} + C_L .$$

However, the squared quantity in brackets in the last expression is much less than unity so that we may write as a close approximation the equality:

$$K = \left\{1 - \left[\frac{1}{(\frac{D}{d})^2 - 1}\right]^2\right\} + C_L . \tag{16}$$

Equation (16) may be used to determine C_L from experimental values of K. For this purpose (16) is written in the form

$$C_L = K + \left\{1 - \left[\frac{1}{(\frac{D}{d})^2 - 1}\right]^2\right\} . \tag{17}$$

Experimental Values of the Loss Coefficient for the Test Apparatus

Values of C_L are calculated in Table II, using Equation (17) and the experimental values of K from Table I. The results are plotted as the solid lines in Fig. 13.

As a check on the above experimental values of C_L, measurements were made of the velocity V_3, area A_3, and pressure p_3 at the lip of the cup for the case D/d = 2.22. The experimental value of the coefficient of pressure loss between points 1 and 3 was computed in a manner similar to that described above for the loss between points 1 and 4. The loss coefficient between points 3 and 4 was then computed using the well known formula (described later) for the loss due to a sudden enlargement of the flow stream, since the flow photographs had indicated that such an enlargement did occur between 3 and 4. The total coefficient between points 1 and 4 was then determined by adding these two losses, and this sum is plotted as the dashed line in Fig. 14. The corresponding values for this case (D/d = 2.22) calculated from Equation (17) are shown in Fig. 14 as a solid line. The experimental values of C_L obtained by the two relatively independent methods agree very closely.

Theoretical Formula for the Loss Coefficient

If C_L can be expressed in terms of known quantities, Equation (16) constitutes a means for predicting the pressure drop in the test apparatus. Known solutions to similar problems, such as that shown in Fig. 15, indicate that in the test apparatus the air stream contracts from points 1 to 2 and attains its minimum area at point 2. Since the maximum area occurs at 4, a possible theoretical formula for the pressure loss is that for a sudden enlargement of the stream from 2 to 4. Such a formula may give the total loss from 1 to 4 if that between 1 and 2 is negligible, as expected in a region of contraction. For these conditions, the sudden enlargement formula may be written

$$p_L = 1/2(\rho V_2^2)\,(1 - A_2/A_4)^2 \quad . \tag{18}$$

Since the volumetric flow is

$$Q = A_1 V_1 = A_2 V_2 \quad , \tag{19}$$

Equation (18) may be written as

$$p_L = 1/2(\rho V_1^2)\,(A_1/A_2)^2\,(1 - A_2/A_4)^2 = 1/2(\rho V_1^2)\,(A_1/A_2 - A_1/A_4)^2 \,. \quad (20)$$

If C_c is called the coefficient of contraction and defined as

$$C_c = A_2/A_1 \quad (21)$$

and if (15) is assumed to be an equality, (20) becomes

$$p_L = 1/2(\rho V_1^2)\left[\frac{1}{C_c} - \frac{1}{\left(\frac{D}{d}\right)^2 - 1}\right]^2 , \quad (22)$$

from (11)

$$C_L = \left[\frac{1}{C_c} - \frac{1}{\left(\frac{D}{d}\right)^2 - 1}\right]^2 \quad (23)$$

The Coefficient of Contraction for a Similar Two-Dimensional Problem and an Ideal Fluid

Figure 15 represents the flow of an ideal (inviscid and incompressible) fluid from a two-dimensional channel against an infinite plane perpendicular to the channel walls. The velocity distribution in the channel is assumed to be constant a long distance upstream from the outlet. The center line of the channel from the stagnation point "0" to infinite values of "y" is a streamline. For an ideal fluid streamlines may be replaced by solid boundaries so a wall is assumed to be located on the centerline and only the right-hand half of Fig. 15 is considered. If, also, the plane barrier makes some general angle α with the channel walls, the problem shown in Fig. 16 arises. When $\alpha = \pi/2$, the flow will be identical with that of the right-hand half of Fig. 15. The coefficient of contraction in this two-dimensional case is then

$$C_c = b/a \quad (24)$$

and may be of interest in the problem since, as shown in Fig. 15, most of the contraction occurs near the channel outlet when α approaches or exceeds 90°.

The coefficient of contraction for the problem of Fig. 16 has been determined theoretically* for values of α from $(1/4)\pi$ to $(3/4)\pi$ (45° to 135°) and is plotted in Fig. 17.

The Coefficient of Contraction for the Axially Symmetric Test Apparatus

In order to use Fig. 17 to obtain C_c for the problem, some relation must be established between the dimensions of the axially symmetric (cylindrical) test apparatus of Fig. 10 and those of the two-dimensional (plane) problem of Fig. 15. The following stipulations can be made for the two cases.

(1) Equality of the initially uniform velocities,

$$V_1 = U_1 \tag{25}$$

(2) Equality of the average of the horizontal component V_o of the velocity through the area $A_h = \pi dh$ (Fig. 1) and the area A_o between the plane barrier and the ends of the channel walls (Fig. 15). That is, since in general

$$V_o = Q/A \ , \tag{26}$$

$$\frac{Q}{A_h} = \frac{V_1 A_1}{A_o} = \frac{V_1(\pi/4)d^2}{\pi dh} = V_1 \left(\frac{d}{4h}\right) \text{ (Fig. 10)} \tag{27}$$

and

$$\frac{Q}{A_o} = \frac{U_1 A_1}{A_o} = U_1 \left(\frac{a}{c}\right) \quad \text{(Fig. 15)} \tag{28}$$

must be equal.

Then by equating (27) and (28)

$$\frac{c}{a} = \frac{4h}{d} \ . \tag{29}$$

*H. Ambrose, University of Iowa Studies in Engineering Bulletin 35 (1953), p.73.

(3) Equality of c and h

$$c = h \quad . \tag{30}$$

By combining (29) and (30)

$$a = d/4 \quad . \tag{31}$$

For any dimension, s, of the two-dimensional problem of perpendicular to the plane in which that figure is drawn, the coefficient of contraction given in Equation (24) is equivalent to the area ratio A_2/A_1, that is,

$$C_c = \frac{b}{a} = \frac{b \cdot s}{a \cdot s} = \frac{A_2}{A_1} \quad . \tag{32}$$

Assume that for Figure 10, also,

$$\frac{A_2}{A_1} = \frac{b}{a} \tag{33}$$

approximately. Then by (21)

$$C_c = b/a \tag{34}$$

for Figure 10, which represents the test apparatus.

Summarizing in Figure 17 a plot of the form

$$b/a = f\,(c/a) \tag{35}$$

with α as a parameter and holding for the two-dimensional problem of Fig. 15 when $\alpha = \pi/2$. By Equations (29) and (30) the data of Fig. 17 may be used to determine C_c for the test apparatus.

Theoretical Values of the Coefficient of the
Pressure Loss in the Cup Region of the Test Apparatus

The theoretical values of C_L are calculated in Table III using Equation (23)

$$C_L = \left[\frac{1}{C_c} - \frac{1}{\left(\frac{D}{d}\right)^2 - 1} \right]^2 , \qquad (23)$$

where

$$C_c = b/a \qquad (34)$$

$$b/a = f\,(c/a) \qquad \text{(Fig. 17)} \qquad (35)$$

$$c/a = 4\,(h/d) \qquad (29)$$

which in effect specify the following relation for the test apparatus.

$$C_L = f\,(h/d,\ D/d) \qquad (36)$$

giving theoretical values of C_L which are plotted as dashed lines in Fig. 13. The experimental values of C_L in Fig. 13 are seen to agree with the theoretical values within limits which are quite satisfactory for air cleaner design purposes.

Having verified the formula (23) for C_L, a completely theoretical expression for the pressure drop in the cup region of the oil spray test apparatus may be written. Substituting (23) in (16),

$$K = 1 - \left[\frac{1}{\left(\frac{D}{d}\right)^2 - 1} \right]^2 + \left[\frac{1}{C_c} - \frac{1}{\left(\frac{D}{d}\right)^2 - 1} \right]^2 \qquad (37)$$

where, by (8) and (10a),

$$\Delta P = p_1 - p_4 = 1/2(\rho V_1^2)K \tag{38}$$

$$V_1 = Q/A_1 \quad . \tag{39}$$

Experimental Values of the Pressure Drop in the Baffle Region of a Production Model Air Cleaner

Figure 11 presents a sectional view of the axially symmetric Donaldson 410-cfm air cleaner. The static gage pressures were measured for a range of flow rates up to 400 cfm at points indicated by circled numbers. This section is concerned with the pressure drop in the baffle region as indicated by the measurements at points a, b1, and b2. Figure 18 shows an enlarged view of the baffle region and also the general character of the flow in this region as observed in model tests.

The experimental values of K corresponding to the pressure drop in the baffle region are calculated in Table IV and plotted in Fig. 19 as solid lines. The presence of oil in the air cleaner is seen to have a negligible effect on the drop in the baffle region. The relatively constant value of K at the higher flows indicates that the rates of flow in the baffle region are sufficiently high so that Reynolds' number is not a factor.

Theoretical Values of the Pressure Drop in the Baffle Region of the Air Cleaner

In Fig. 18 the velocity is known to be essentially uniform over the cross sections of 1 and 2 for the same reasons as given for the corresponding points of the test apparatus. The flow leaving the first screen was observed to be uniform in the water channel tests of two-dimensional models. Consequently, the velocity V_4 is taken as uniform over the upstream surface of the first screen. Specifically, the velocity V_4 is assumed to be uniform over an area A_4 consisting of the total area of the stream as it passes through the upstream (first) layer of the screens comprising the first screen region. Station 4 is taken in the first layer since this is the only point of the main stream in this locality at which a uniform velocity distribution is likely. The pressure measured at point b2 (or b1) is assumed to have the same value as p_4, a constant pressure over the area A_4.

The formula for the pressure drop between 1 and 4 may be obtained in the manner demonstrated above in the analysis of the test apparatus.

$$K = \frac{p_1 - p_4}{1/2(\rho V_1^2)} = \left[1 - \left(\frac{A_1}{A_2}\right)^2\right] + C_L \qquad (40)$$

The pressure-loss formula (20) will also apply:

$$p_L = 1/2(\rho V_1^2)\,(A_1/A_2 - A_1/A_4)^2 \; ; \qquad (20)$$

and since C_L is defined by (11) as

$$p_L = C_L\,(1/2\rho V_1^2) \; , \qquad (41)$$

we have

$$C_L = \left(\frac{A_1}{A_2} - \frac{A_1}{A_4}\right)^2 = \left(\frac{1}{C_c} - \frac{A_1}{A_4}\right)^2 \; , \qquad (42)$$

where C_c is still determined by Fig. 17 and the set of equations [(34), (35), and (29)] which are listed together on page 9. Then (40) becomes

$$K = \left[1 - \left(\frac{A_1}{A_4}\right)^2\right] + \left[\frac{1}{C_c} - \frac{A_1}{A_4}\right]^2 \; . \qquad (43)$$

If A_4' is the gross annular area of the first screen region (the area at 4 which is open to flow if the screens of the first region are removed), and if C_4 is the fraction of A_4' which is open (i.e., which is not occupied by the wire of the first layer of screen, the area open to flow in this layer is C_4A_4'. If, then, C_{c4} is the coefficient of contraction of the portion of the stream through any one opening of the first layer, the area of the total stream at station 4 is

$$A_4 = C_{c4}\,C_4A_4' \qquad (44)$$

and

$$\frac{A_1}{A_4} = \frac{1}{C_{c4}\, C_4}\left(\frac{A_1}{A_4'}\right) . \tag{45}$$

Utilizing the area theorem of Pappus* to determine A_4', we obtain

$$\frac{A_1}{A_4'} = \frac{d^2}{(2/\sqrt{3})(D_a^2 - D_d^2)} = \frac{\sqrt{3}}{2}\left[\frac{1}{\left(\frac{D_a}{d}\right)^2 - \left(\frac{D_d}{d}\right)^2}\right] , \tag{46}$$

which for the dimensions of Fig. 18 becomes

$$\frac{A_1}{A_4'} = 0.211 . \tag{47}$$

In the Donaldson 410-cfm air cleaner, the first screen region consists of layers of 14-mesh screen of 0.0165-in.-diameter wire. For this material, C_4 is readily computed to be

$$C_4 = 0.5914 . \tag{48}$$

The coefficient of contraction C_{c4} is given with sufficient accuracy by that for a sharp edge, circular orifice in a round pipe. The coefficient for the latter case is essentially the discharge coefficient plotted in Fig. 20** against the square root of the Reynolds' number with the ratio of orifice diameter to pipe diameter as a parameter. For the flow through the first layer of the first screen region the value of this parameter may be taken as

$$\frac{k}{m} = \frac{m - n}{m} = \frac{0.0714 - 0.0165}{0.0714} = 0.77 \tag{49}$$

*Mechanical Engineers' Handbook, L. S. Marks (editor), 4th edition, 1941, p. 111 (listed as the second theorem of Pappus in this reference).

**H. Rouse, Fluid Mechanics for Hydraulic Engineers, First Edition, McGraw-Hill Book Company Inc., New York, 1938, p. 260.

where m is the distance between the axes of parallel wires, n is the wire diameter, and k is the length of a side of an individual square opening in the screen. The Reynolds' number may be estimated as

$$R = \frac{V_4 k'}{\nu} = \frac{4Q}{\pi (k')^2} \frac{k'}{\nu} \cong \frac{4Q}{\pi k \nu} \tag{50}$$

where k' is the diameter of a circle of area k^2. If

$$Q = 100 \text{ ft}^3/\text{min} = (100/60) \text{ ft}^3/\text{sec} ,$$

$$k = 0.0714 - 0.0165 = 0.0549 \text{ in.} = 0.0549/12 \text{ ft, and}$$

$$\nu = 18.5 \times 10^{-5} \text{ ft}^2/\text{sec} \quad \text{(kinematic viscosity for air at 60°F and 29.5" Hg)} ,$$

then

$$R = 2{,}509{,}000 \text{ at } 100 \text{ cfm} \tag{51}$$

and

$$\sqrt{R} = 1{,}548 \text{ at } 100 \text{ cfm.}$$

This high value of R at only 25 percent of the maximum flow indicates (Fig. 20) that C_{c4} is independent of the Reynolds' number. Using the value in (49), and consulting the portion of Fig. 20 corresponding to high values of R,

$$C_{c4} \cong 0.63 . \tag{52}$$

Substituting (47), (48), and (52) in (45),

$$\frac{A_1}{A_4} = \frac{1}{(0.5914)(0.63)} (0.211) = 0.566 \tag{53}$$

and

$$\left(\frac{A_1}{A_4}\right)^2 = 0.321 . \tag{54}$$

From the dimensions of Fig. 18, we obtain

$$h/d = 0.36 \tag{55}$$

whence by (29)

$$c/a = 4\,(h/d) = 1.44 \tag{56}$$

and by Figure 17

$$C_c = b/a = 0.663\,, \tag{57}$$

so that

$$1/C_c = 1.51\,. \tag{58}$$

Then substituting (53), (54), and (58) into (43),

$$K = (1 - .321) + (1.51 - .566)^2 = 1.56\,. \tag{59}$$

This computed value of K is plotted as a dashed line in Fig. 19 where, at the higher flows, it can be seen to be in essential agreement with the experimental values. Equations (42) and (43) originally derived for the test apparatus, are now verified for the air cleaner.

Minimum Pressure Loss in the Baffle Region

For the test apparatus, use was made of the relation

$$\frac{A_1}{A_4} = \frac{\pi/4\ d^2}{\pi/4\ (D^2 - d^2)} = \frac{1}{(D/d)^2 - 1}\,. \tag{60}$$

To permit comparison of C_L for the test apparatus and air cleaner, let (60) define D/d in the latter case. Thus, by (53) and (60)

$$0.566 = \frac{1}{\left(\frac{D}{d}\right)^2 - 1} \tag{61}$$

and

$$(D/d)^2 = 2.767, \quad D/d = 1.663 . \tag{62}$$

Using this value of D/d, the theoretical value of the loss coefficient C_L of the cleaner is calculated from Equation (42) as a function of h/d (Table V) and plotted in Fig. 21. The value of C_L for the present design of the baffle region is, according to Equation (55), that corresponding to h/d = 0.36. That is, $C_L = 0.89$. The theoretical values of C_L for other values of D/d are also plotted in Fig. 21 and have been taken from Fig. 13.

Comparing the experimental values of C_L in Fig. 13 for the test apparatus, we see that the data suggest the existence of minimum values of C_L for certain values of h/d. By Equation (43) these points will correspond to the minimum possible values of K, and thus of the pressure drop, for a given value of A_1/A_4 (i.e., of D/d). The experimentally determined minimum values of C_L are plotted against D/d in Fig. 22.

From Equation (42) it can be seen that the minimum value of C_L will correspond to a maximum value of C_c which approaches the limit unity as h/d (that is, c/a) increases in Fig. 17. These theoretical minimum values of C_L are calculated in Table VI and are plotted in Fig. 22 against the ratio D/d representing the range of A_1/A_4 of interest.

It is apparent from Fig. 21 that the value of $C_L = 0.89$ for the present design of the air-cleaner baffle region will decrease rapidly as h/d is increased above its present value of 0.36. A further improvement will result (Fig. 22) from decreasing the ratio D/d, that is, from increasing the value of A_1/A_4, if practicable.

Distribution of Pressure Drop and Flow in Various Regions of the Donaldson Air Cleaner

The pressure was measured at seven stations in the Donaldson 410-cfm air cleaner (Fig. 11) for various air flow rates with and without oil in the cleaner. When oil was present in the cleaner, the manometer connection was tied into a bubbler, and an extremely low rate of air flow was allowed to pass through the manometer tap into the air cleaner. The bubbler permitted observation of the flow and thus a continuous check against plugging of the line by oil. There was no indication of plugging at any time and, as shown in Fig. 23, pressure drops measured with oil present agreed well with measurements made in the absence of oil except in the main screen region where such agreement was not to be expected.

Table VII summarizes the pressure measurements obtained. Table VIII gives the pressure drops in the entry, baffle, main screen, and discharge regions of the cleaner, as computed from the pressure measurements of Table VII. In the following discussion, attention is devoted primarily to the maximum pressure drops (occurring at the maximum flow), since these are an important factor in design.

Effect of Oil on Pressure Drop

The average pressure drops in the various regions are plotted in Fig. 23. At the larger flows where the higher pressure drops are encountered, the data covers tests both with and without oil. At the maximum flow, the presence of oil is seen to have a significant effect on pressure drop only in the main screen region where it causes an increase of 500 percent. The corresponding increase of pressure drop in the baffle region is only 12 percent.

Comparison of Pressure Drop in Various Regions

In Fig. 23 it is seen that, in the presence of oil and at maximum flow, the pressure drops are about equal in the baffle, main screen, and discharge regions. However, the drop in the entry region is much larger and, in fact, is 4.8 inches of water or about 60 percent of the total drop through the cleaner.

The pressure drop in the baffle region has been analyzed above. The pressure drop in the main screen and discharge regions is discussed below in connection with the circumferential distribution of flow.

The large drop in the entry region was anticipated from the study of two-dimensional models in the water channel. As noted in Chapter III, the drop in the entry region can be substantially reduced by the addition of a ring-type vane to divert flow through the space at the upper end of the down tube, which is now occupied by an elongated toroidal eddy. This change may be effected as a modification of the present design of the entry region, but a redesign of this region may be preferable from a manufacturing standpoint. In either case, it appears that the present entry baffle may remain unchanged if so desired.

Circumferential Distribution of Flow

As can be seen in Fig. 11, the pressure-measurement stations in the Donaldson air cleaner were selected so as to obtain an indication of the amount of non-uniformity in the distribution of the air flow around the axis of the cleaner. The pressure drops with oil present are plotted in Fig. 24 for both the outlet side of the cleaner (side 1) and the opposite side (side 2).

The flow on the two sides appears to be quite uniform except in the discharge region, where a marked non-uniformity appears to exist. Here the pressure drop on side 1 is seen to exceed that on side 2 by a factor of 10. This condition indicates that in the discharge region the flow on side 1 may be more than 3 times that at 2, since the average drop in this region varies approximately as the square of the rate of air flow. Such a non-uniformity would represent a considerable overloading of the screen in the discharge region near side 1 and underloading elsewhere in this region.

In the present design, the outlet restriction has been intentionally varied around the discharge region, decreasing from side 1 toward side 2. Also, a top view of the cleaner would show that the centerline of the outlet nipple of the air cleaner is not located in a radial plane of the air cleaner, but is eccentric, presumably in order to induce in the outlet manifold a unidirectional circulatory flow about the axis of the cleaner. The varying restriction and eccentric outlet should promote uniformity of flow in the discharge region. However, it appears that they are inadequate for this purpose, at least as now incorporated in the design of the cleaner.

Presumably, a more uniform flow could be obtained by adopting a more drastic variation of the outlet restriction from side 1 to 2, even at the expense of increasing the average pressure drop in the discharge region.

Furthermore, any increase in pressure differential may be more offset by the proposal for decreasing the drop in the entry region. An alternative and preferable solution may lie in moderately increasing the variation of the outlet restriction and also effecting a general re-shaping of the outlet manifold which as now designed is not conductive to a stable pattern of the flow within it. It may also be necessary to restrict circumferential flow in the screen of the discharge region by some means such as that described next.

It is assumed that the placing of vertical guide vanes at various radial positions in the discharge region is undesirable from a manufacturing standpoint. In the case of the Donaldson air cleaner, the screen in this region consists of 26 turns of crimped, 12-mesh screen of 0.0105-inch-diameter wire. This screen differs from that used elsewhere in the cleaner. By virtue of the observed non-uniformity which exists solely in the discharge region, the screen used here must permit considerable circumferential flow as the air stream approaches the outlet restriction. Since this tangential component of flow is not of the unidirectional, circulatory type apparently intended, a different type of screen in the discharge region which discourages all circumferential flow may give improved results. Such a screen would act in the same manner as radial guide vanes without introducing the practical problems caused by the latter. In this manner, the uniform flow now existing in the baffle and main screen regions (Fig. 23) would tend to persist in the discharge region.

Conclusions

The study of the cup region of the test apparatus and the baffle region of the Donaldson 410-cfm air cleaner provides some insight into the behavior of the air flow in these sections. The theoretical equation (38) is shown (Fig. 13) to adequately relate the pressure drop, the rate of flow, and the dimension ratios (h/d and D/d) of the test apparatus for a considerable range of the latter ratios. The equation is also shown (Fig. 19) to be applicable, at the higher rates of flow, to the baffle region of the Donaldson cleaner. In view of this verification over a considerable range of size and form of the flow boundaries, Equation (38) can be expected to apply to the corresponding region of other sizes and models of air cleaners.

The application of these results to baffle region design is then illustrated for the Donaldson cleaner. It is shown that in the case of this cleaner the coefficient of pressure loss, C_L, can be decreased considerably by increasing (h/d) slightly (Fig. 21) and also, if practical, by decreasing (D/d) (Fig. 22). In general, if one of the set of dimensions h, d, or D (or the equivalent set h, A_1, and A_4) is specified, the analysis provides a guide

in selecting the values of the others which will yield a minimum pressure loss in the baffle region.

To illustrate a method of analyzing other regions of an air cleaner, attention is then given to the distribution of the pressure drop and flow in the various regions of the Donaldson air cleaner, as indicated by pressure measurements at various points in the cleaner. The following conclusions are indicated by the data:

1. The relation between the average pressure drop and the rate of air flow is essentially unaffected by the presence or absence of oil in the cleaner except in the main screen region, where a large effect is observed (Fig. 23). Consequently, an analysis of the air flow in the absence of oil, such as that carried out for the baffle region, would be ineffective in the main screen region but could be expected to be possible for the entry and discharge regions. However, such an analysis in the latter regions offers but limited usefulness, since the various cleaners differ substantially in the geometry of their entry and discharge sections. Furthermore, as noted below, the measures for reducing the pressure drop in these regions can be determined merely by observation of the flow pattern.

2. The average pressure drops in the baffle, main screen (with oil present), and discharge regions are about equal (Fig. 23). Consequently, the possible reductions in the baffle pressure drop already noted (Figs. 21 and 22), would permit increasing the density of wire in the main screen region, if desired, without increasing the overall pressure drop in the cleaner.

3. The average pressure drop is largest in the entry region (Fig. 23) where it is about 60% of the total drop through the cleaner. Means for reducing this drop are suggested by the study of the photographs of the flow in the entry region and are discussed in this chapter.

4. The pressure-drop measurements on the outlet side (side 1) of the cleaner and on the opposite side (side 2) are plotted in Fig. 24. The data indicate that the flow in the baffle and main screen regions is of uniform circumferential distribution, but the flow on side 1 of the discharge region is several times that on side 2. Several possible solutions have been suggested in this chapter.

In general, the analytical study proved desirable in some regions and not in others. However, it is seen that in a problem with abrupt changes in the dimensions of the flow boundaries, such as in the air cleaner, it is always necessary to have advance knowledge of the general shape of the main air stream and eddy regions whether or not an analytical study is made. With

experience, the stream and eddy pattern can be predicted in simple cases, but in general such a procedure is unreliable. It is also unnecessary to attempt predictions of this kind in view of the ease and effectiveness with which the water channel and two-dimensional models can be used to study the flow pattern. The study of air cleaner models in the water channel is described in Chapter III of this report.

TABLE I

EXPERIMENTAL VALUES OF THE PRESSURE DROP IN THE TEST APPARATUS

$$K = \frac{\Delta P}{\frac{1}{2}\rho V_1^2} \quad ; \quad \Delta P = p_1 - p_4$$

① Item	② D/d	③ h/d	④ A_h/A_1 (4h/d)	⑤ A_4/A_1 $(\frac{D}{d})^2 - 1$	⑥ A_h/A_4 ④/⑤	⑦ ΔP (in. H_2O)	⑧ Q (scfh)	⑨ K	⑩ Reg. No. (Q/d) (ft^2/sec)	⑪ H/d	⑫ h/H ③/⑪	⑬ l/d	⑭ d (in.)
1	2.00	.125	.500	3.000	.1665	13.20	4,000	7.01	8.89	1.33	.0938	14.00	1.50
2		.333	1.333		.4439	1.07		5.68			.250		
3		.500	2.000		.6660	- .08		- .042			.375		
4		.916	3.664		1.220	- .49		- .263			.687		
5		1.000	4.000		1.333	- .48		- .255			.750		
6		1.250	5.000		1.667	.00		.000			.938		
7	2.22	.111	.444	3.928	.113	8.40	6,000	10.00	8.89	1.11	.100	9.33	2.25
8		.333	1.333		.339	.72		.860			.300		
9		.500	2.000		.509	.16		.191			.450		
10		.611	2.444		.622	.00		.000			.550		
11		.777	3.108		.791	- .15		- .179			.700		
12		.833	3.332		.848	- .12		- .143			.750		
13		1.000	0.000		1.018	- .18		- .215			.901		
14	2.66	.125	.500	6.076	.082	17.75	4,000	9.430	8.89	1.00	.125	14.00	1.50
15		.333	1.333		.219	1.20		.637			.333		
16		.584	2.336		.385	.02		.010			.584		
17		.666	2.664		.438	- .10		- .053			.666		
18		.916	3.664		.603	- .32		- .170			.916		
19		1.000	4.000		.658	- .38		- .202			1.000		
20		1.333	5.333		.878	- .11		- .058			1.333		

TABLE I (cont.)

(1) Item	(2) D/d	(3) h/d	(4) A_h/A_1 (4h/d)	(5) A_4/A_1 $(\frac{D}{d})^2 - 1$	(6) A_h/A_4 (4/5)	(7) ΔP (in. H_2O)	(8) Q (scfh)	(9) K	(10) Reg. No. (Q/d) (ft^2/sec)	(11) H/d	(12) h/H (3/11)	(13) l/d	(14) d (in.)
21	3.33	.125	.500	10.089	.050	20.00	4,000	10.62	8.89	1.66	.0753	14.00	1.50
22		.333	1.333		.132	1.83		.956			.201		
23		.666	2.664		.264	- .02		- .010			.401		
24		1.250	5.000		.496	- .39		- .207			.753		
25		1.416	5.664		.561	- .39		- .207			.853		
26		1.666	6.664		.660	- .30		- .159			1.004		
27		1.750	7.000		.694	- .24		- .127			1.054		

Note: Flowing fluid: Air at 70°F and 29.3 inches Hg.
Flow rates (Q) in scfh (ft^3/hr at standard temp. and pressure).
Column 4: A_h is defined as (πdh).
Column 9: K is defined as ($\Delta P/1/2\ \rho\ V_1^2$), where ΔP is in lb/ft^2
V_1 in ft/sec and ρ in slugs/ft^3. For units of col. 7, 8, and 14,
$K = (1.69 \times 10^6)\ d^4\ (\Delta P/Q^2)$.
Column 10: Q/d is proportional to the Reynolds' No. For the Donaldson cleaner
Q/d = 18.22 ft^2/sec at 410 cfm.

TABLE II

EXPERIMENTAL VALUES OF COEFFICIENT OF PRESSURE LOSS IN TEST APPARATUS

$$C_L = K + \left[1 - \left(\frac{1}{\frac{D^2}{d^2} - 1}\right)^2\right]$$

(1) D/d	(2) h/H	(3) h/d	(4) $(D/d)^2$	(5) (4)-1	(6) 1/(5)	(7) (6)^2	(8) 1-(7)	(9) K	(10) (8)+(9)	(11) Ah/A_4
2.00	.0938	.125	4.	3.	.3333	.1111	.8889	7.01	7.899	.167
	.250	.333						.568	1.457	.444
	.375	.500						- .042	.847	.667
	.687	.916						- .263	.626	1.221
	.750	1.000						- .255	.634	1.333
	.938	1.250						.000	.889	1.667
2.22	.100	.111	4.928	3.928	.2546	.0648	.9352	10.00	10.94	.113
	.300	.333						.860	1.795	.339
	.450	.500						.191	1.126	.509
	.550	.611						.000	.935	.622
	.700	.777						- .179	.756	.791
	.750	.833						.143	.792	.848
	.901	1.000						.215	.720	1.018
2.66	.125	.125	7.076	6.076	.1646	.02708	.97292	9.430	10.403	.082
	.333	.333						.637	1.610	.219
	.584	.584						.010	.983	.385
	.666	.666						- .053	.920	.438
	.916	.916						- .170	.803	.603
	1.000	1.000						- .202	.771	.658
	1.333	1.333						- .058	.915	.878
3.33	.075	.125	11.089	10.089	.0991	.0098	.9902	10.620	11.610	.050
	.201	.333						.956	1.946	.132
	.401	.666						- .010	.980	.264
	.753	1.250						- .207	.783	.496
	.883	1.466						- .207	.783	.561
	1.004	1.666						- .159	.831	.660
	1.054	1.750						- .127	.863	.694

TABLE III

THEORETICAL VALUES OF COEFFICIENT OF PRESSURE LOSS IN TEST APPARATUS

$$C_L = \left[\frac{1}{C_c} - \frac{1}{\left(\frac{D}{d}\right)^2 - 1}\right]^2$$

① D/d	② h/d	③ c/a 4 x ②	④ C_c (Fig. 8)	⑤ $1/C_c$	⑥ $\left[\left(\frac{D}{d}\right)^2 - 1\right]^{-1}$	⑦ ⑤ - ⑥	⑧ ⑦²
2.00	.125	.500	.27	3.704	.3333	3.337	11.14
	.333	1.333	.63	1.587		1.254	1.573
	.500	2.000	.813	1.230		.897	.805
	.916	3.664	.975	1.026		.693	.480
	1.000	4.000	.985	1.015		.682	.465
	1.250	5.000	.996	1.004		.671	.450
2.22	.111	.444	.26	3.846	.2546	3.591	12.90
	.333	1.333	.63	1.587		1.332	1.774
	.500	2.000	.813	1.230		.975	.951
	.611	2.444	.875	1.143		.888	.789
	.777	3.108	.938	1.066		.811	.658
	.833	3.332	.956	1.046		.791	.626
	1.000	4.000	.985	1.015		.760	.578
2.66	.125	.500	.27	3.704	.1646	3.539	12.52
	.333	1.333	.63	1.587		1.422	2.022
	.584	2.336	.863	1.159		.994	.988
	.666	2.664	.900	1.111		.946	.895
	.916	3.664	.975	1.026		.861	.741
	1.000	4.000	.985	1.015		.850	.723
	1.333	5.333	.997	1.003		.838	.702
3.33	.125	.500	.27	3.704	.0991	3.605	13.00
	.333	1.333	.63	1.587		1.488	2.214
	.666	2.664	.900	1.111		1.012	1.024
	1.250	5.000	.996	1.004		.905	.819
	1.466	5.864	1.000	1.000		.901	.812
	1.666	6.664	1.000	1.000		.901	.812
	1.750	7.000	1.000	1.000		.901	.812

Note:

Column 4: C_c is the value of b/a determined from Fig. 8.

Column 6: Values taken from column 6 of Table II.

TABLE IV

EXPERIMENTAL VALUES OF THE PRESSURE DROP
IN THE AIR CLEANER BAFFLE REGION

$$K = \frac{\Delta P}{\frac{1}{2}\rho V_1^2} \quad , \quad \Delta P = p_1 - p_4$$

①	②	③	④	⑤	⑥	⑦	⑧	⑨	⑩	⑪	⑫
				Without Oil				With Oil			
Dc/d	h/d	Orif Comb	Q (scfm)	p_1	p_4	ΔP	K	p_1	p_2	ΔP	K
1.33	.36	I	50	- .12	- .125	.005	.384				
			70	- .19	- .22	.03	1.176				
			100	- .35	- .42	.07	1.344				
			150	- .75	- .91	.16	1.365				
		II	150	- .96	-1.12	.16	1.365	- .91	-1.31	.40	3.413
			200	-1.42	-1.70	.28	1.344	-1.35	-1.80	.45	2.160
			300	-3.04	-3.63	.59	1.259	-2.86	-3.48	.62	1.323
			400	-5.10	-6.18	1.08	1.296	-4.80	-6.00	1.20	1.440

Note:

Column 3: I and II indicate two different orifice combinations used to measure the air flow over the range of 50 to 400 cfm. A slight overlap error can be seen above, but is not important in this problem.

Columns 5 and 6: p_1 and p_4 are, respectively, the gauge pressure measured at station a and the average of the pressures measured at b1 and b2.

Columns 8 and 12: For the units of columns 4, 7, and 10, K is given by

$$K = 468\, d^4\, (\Delta P/Q^2) = 192 \times 10^3\, (\Delta P/Q^2) ,$$

where d is in inches (d = 4.5 inches).

All pressures in columns 5, 6, 7, 9, 10, and 11 are in inches of water.

TABLE V

THEORETICAL VALUES OF
COEFFICIENT OF PRESSURE LOSS IN AIR CLEANER

$$C_L = \left[\frac{1}{C_c} - \frac{A_1}{A_4}\right]^2$$

① D/d	② h/d	③ c/a 4 x ②	④ C_c Fig.8	⑤ $1/C_c$	⑥ A_1/A_4	⑦ ⑤ - ⑥	⑧ ⑦^2
1.66	.125	.500	.270	3.704	.566	3.138	9.847
	.333	1.333	.630	1.587		1.021	1.042
	.360	1.440	.663	1.510		.944	.891
	.500	2.000	.813	1.230		.664	.441
	.916	3.664	.975	1.026		.460	.212
	1.000	4.000	.985	1.015		.449	.202
	1.250	5.000	.996	1.004		.438	.192

TABLE VI

THEORETICAL MINIMUM VALUES C_L
FOR TEST APPARATUS AND AIR CLEANER

$$C_L = \left[\frac{1}{C_c} - \frac{A_1}{A_4}\right]^2 \geqq \left[1 - \frac{A_1}{A_4}\right]^2$$

① D/d	② A_1/A_4	③ 1 - ②	④ ③^2
1.66	.5660	.4340	.188
2.00	.3333	.6667	.444
2.22	.2546	.7454	.556
2.66	.1646	.8354	.698
3.33	.0991	.9009	.812

TABLE VII

EXPERIMENTAL VALUES OF THE PRESSURE AT VARIOUS POINTS IN THE AIR CLEANER

Station	Oil	Pressure (inches of water)							
		Orifice Combination I				Orifice Combination II			
		Q = 50	70	100	150	150	200	300	400
a	w/o	.12	.19	.35	.75	.96	1.42	3.04	5.10
b1		.12	.22	.42	.90	1.08	1.70	3.66	6.15
b2		.13	.22	.42	.92	1.16	1.70	3.60	6.20
c1		.15	.25	.45	.95	1.19	1.80	3.80	6.35
c2		.16	.25	.43	.96	1.19	1.75	3.77	6.35
d1		.20	.32	.60	1.25	1.50	2.42	5.10	8.65
d2		.17	.27	.47	1.01	1.22	1.80	3.90	6.45
a	with					.91	1.35	2.86	4.80
b1						1.30	1.77	3.46	6.00
b2						1.32	1.82	3.50	6.00
c1						1.50	2.08	4.20	7.10
c2						1.49	2.07	4.20	7.00
d1						1.85	2.67	5.50	9.20
d2						1.50	2.12	4.28	7.20

Note: All pressures are in inches of water of vacuum below the atmospheric pressure at the inlet of the air cleaner. Flow rates (Q) are given in scfm (ft^3/min. of air at standard temperature and pressure).

TABLE VIII

EXPERIMENTAL VALUES OF THE PRESSURE DROP
IN VARIOUS REGIONS OF THE AIR CLEANER

Region	Points	Oil	Pressure Drop (Inches of Water) Q=50	70	100	150	150	200	300	400
Entry	inlet to a	w/o	.12	.19	.35	.75	.96	1.42	3.04	5.10
Baffle	a to b1		.00	.03	.07	.15	.12	.28	.62	1.05
	a to b2		.01	.03	.07	.17	.20	.28	.56	1.10
	average		.00	.03	.07	.16	.16	.28	.59	1.07
Screen	b1 to c1		.03	.03	.03	.05	.11	.10	.14	.20
	b2 to c2		.03	.03	.01	.04	.03	.05	.17	.15
	average		.03	.03	.02	.04	.07	.07	.15	.17
Discharge	c1 to d1		.05	.07	.15	.30	.31	.62	1.30	2.30
	c2 to d2		.01	.02	.04	.05	.03	.05	.13	.10
	average		.03	.04	.09	.17	.17	.33	.71	1.20
Entry	inlet to a	with					.91	1.35	2.86	4.80
Baffle	a to b1						.39	.42	.60	1.20
	a to b2						.41	.47	.64	1.20
	average						.40	.44	.62	1.20
Screen	b1 to c1						.20	.31	.74	1.10
	b2 to c2						.17	.25	.70	1.00
	average						.18	.28	.72	1.05
Discharge	c1 to d1						.35	.59	1.30	2.10
	c2 to d2						.01	.05	.08	.20
	average						.18	.32	.69	1.16

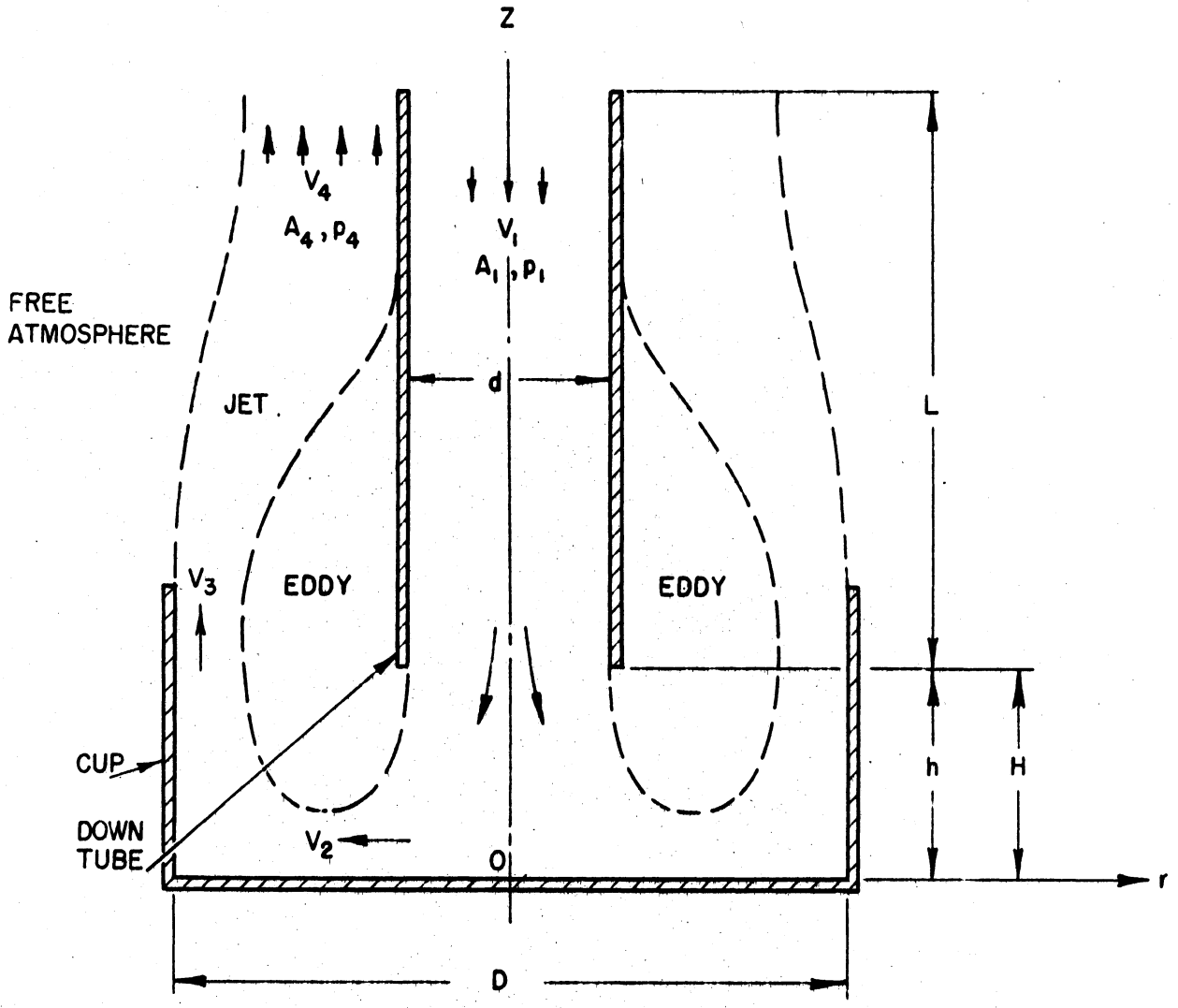

Fig. 10. The observed character of the air flow through the cup region of the axially symmetric oil-spray test apparatus.

Symbols:

$\Delta p = p_1 - p_4$

$R = \frac{V_1 d}{\nu}$

$\nu = \frac{\mu}{\rho}$

μ = absolute viscosity of air

ρ = mass density of air

V = velocity

A = area

ϕ = pressure

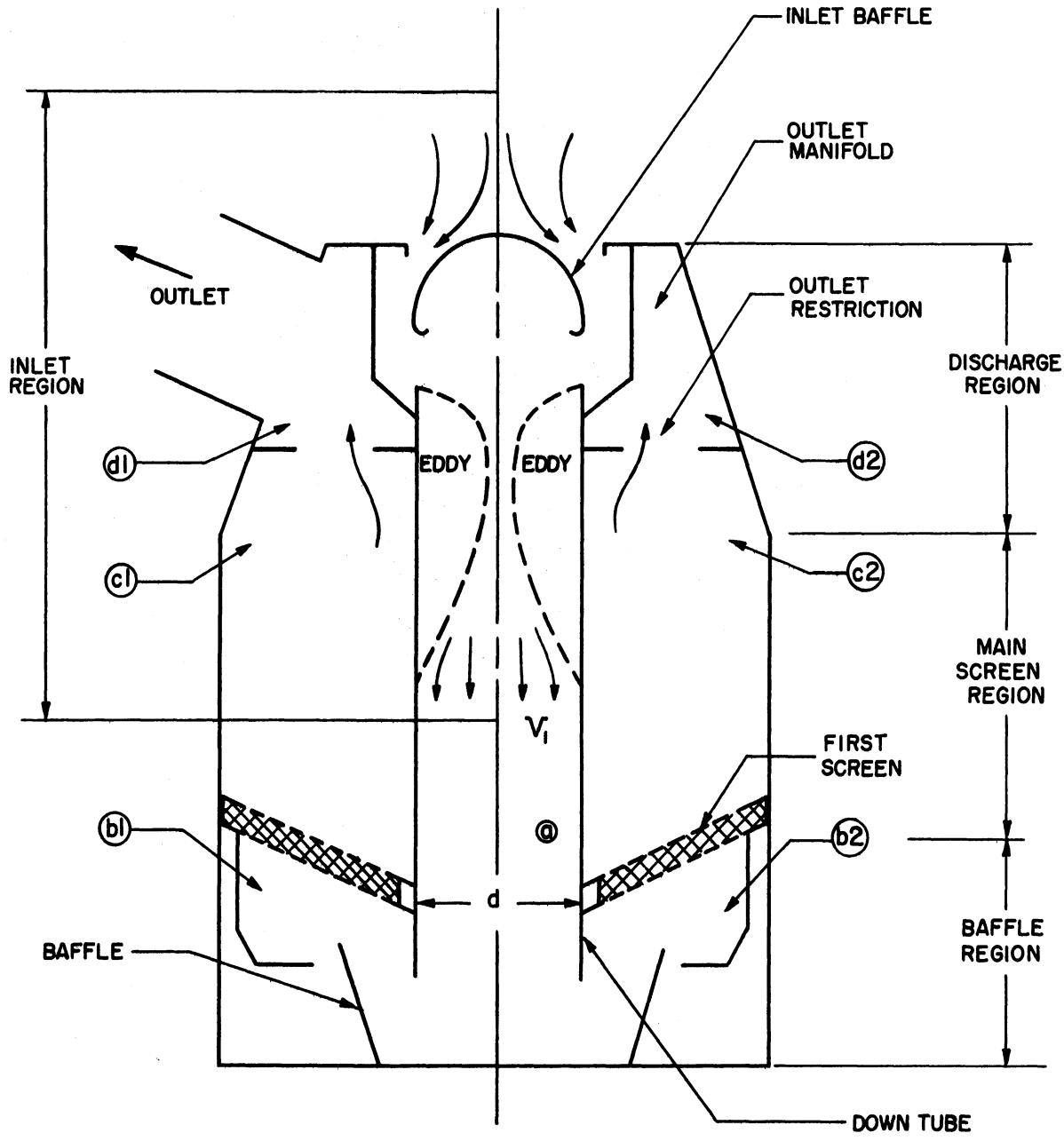

Fig. 11. Diametral section of the axially symmetric Donaldson (400 cfm) air cleaner. Points at which the pressure was measured are indicated by circled numbers.

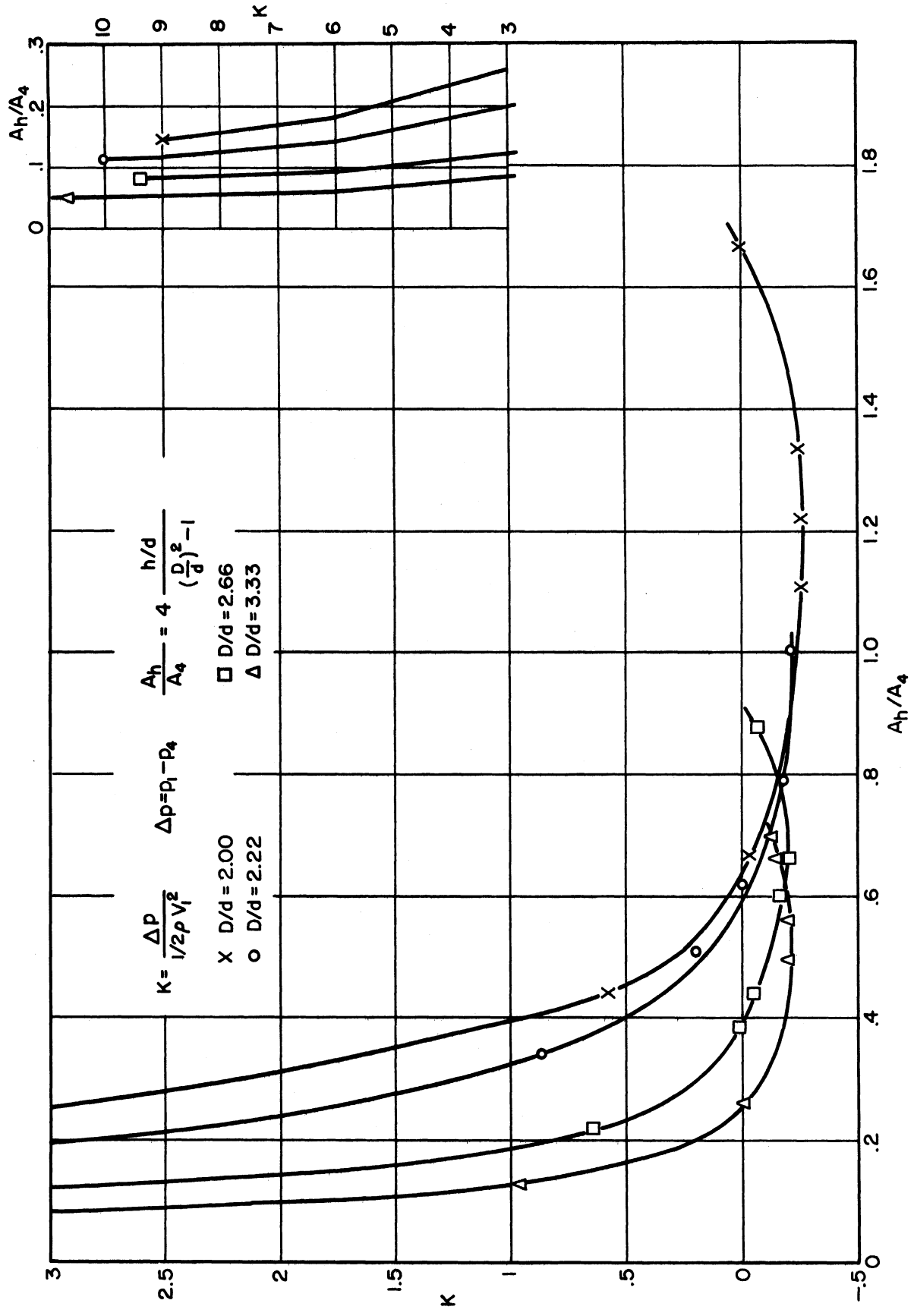

Fig. 12. Experimental values of the pressure drop in the test apparatus.

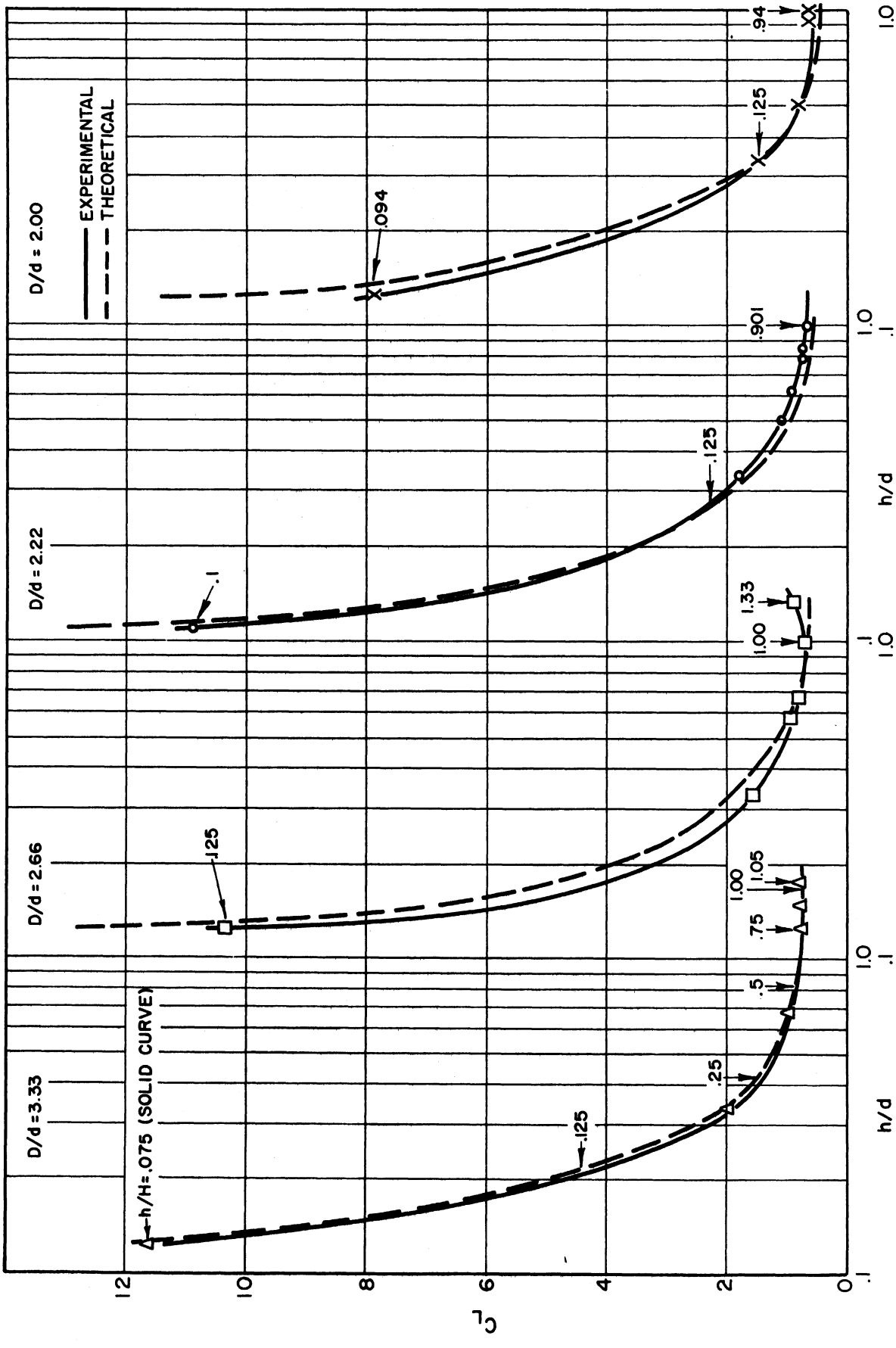

Fig. 13. Experimental and theoretical values of C_L in test apparatus.

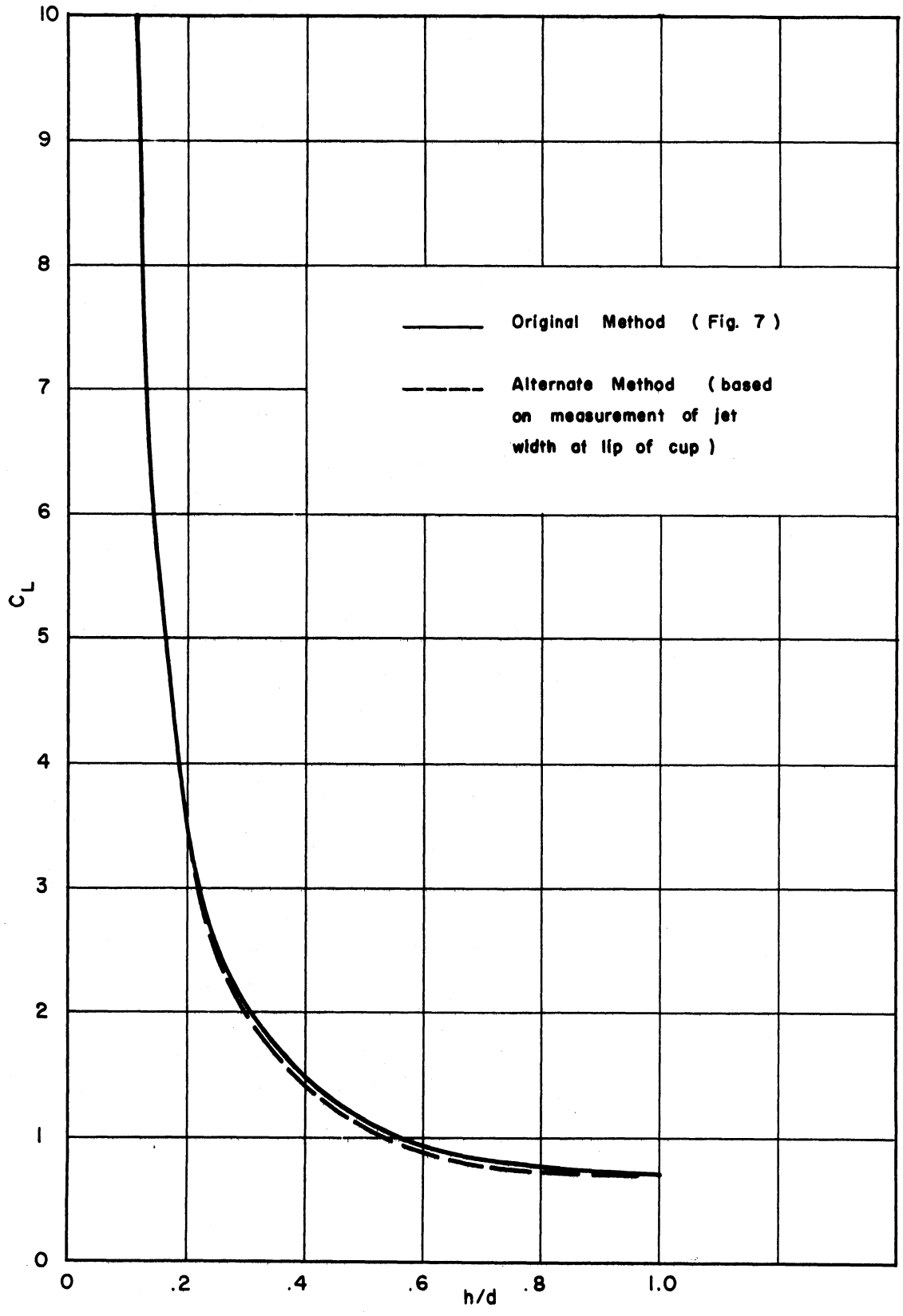

Fig. 14. Comparison of experimental values of C_L obtained by independent methods for D/d = 2.22.

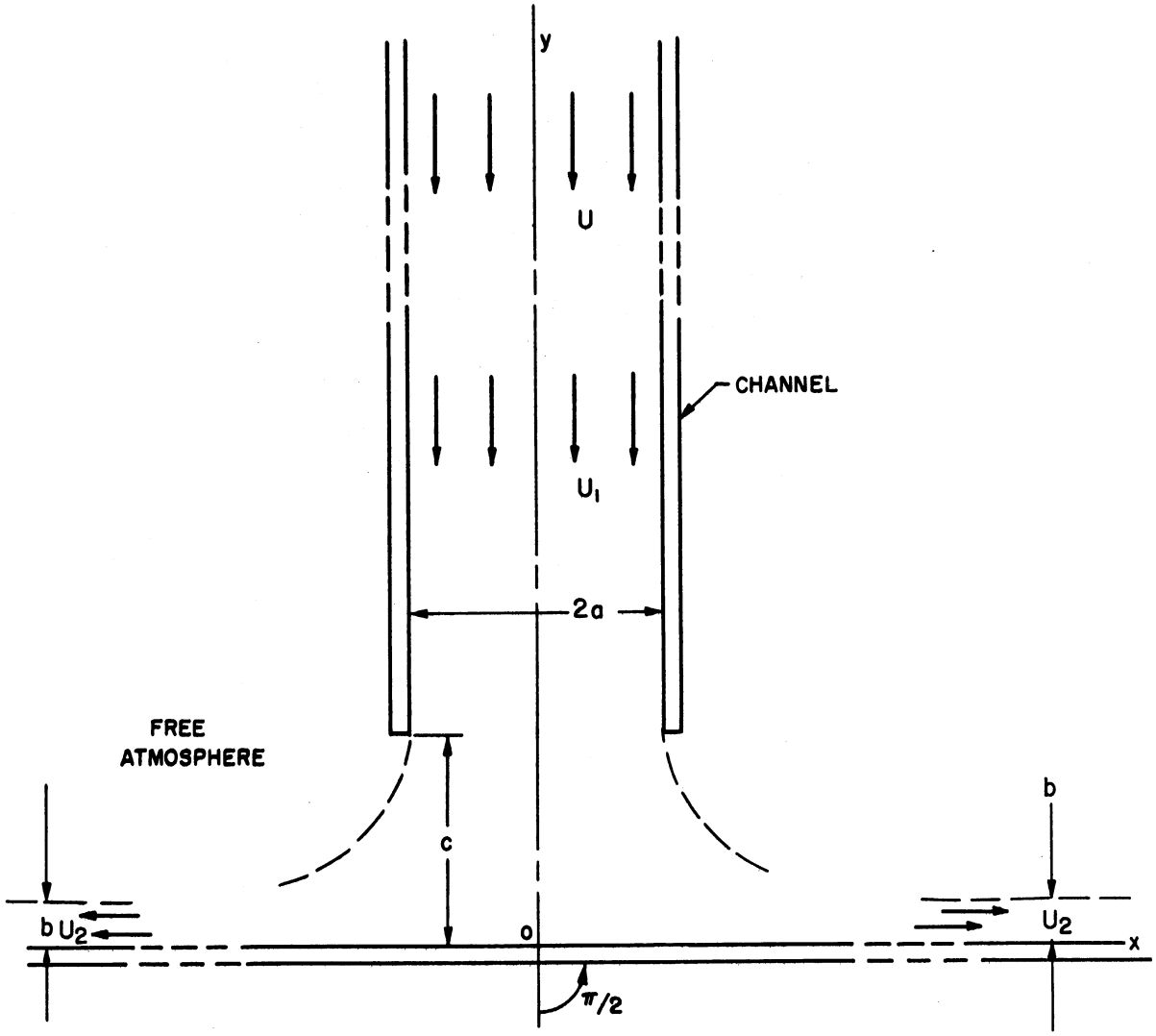

Fig. 15. The theoretical character of the flow of an incompressible, inviscid fluid in the case of the efflux from a two-dimensional channel against an infinite plane barrier perpendicular to the channel. U is the velocity for very large values of y and is assumed uniform across the channel. U_1 is the velocity a short distance above the channel outlet and is not uniform in general.

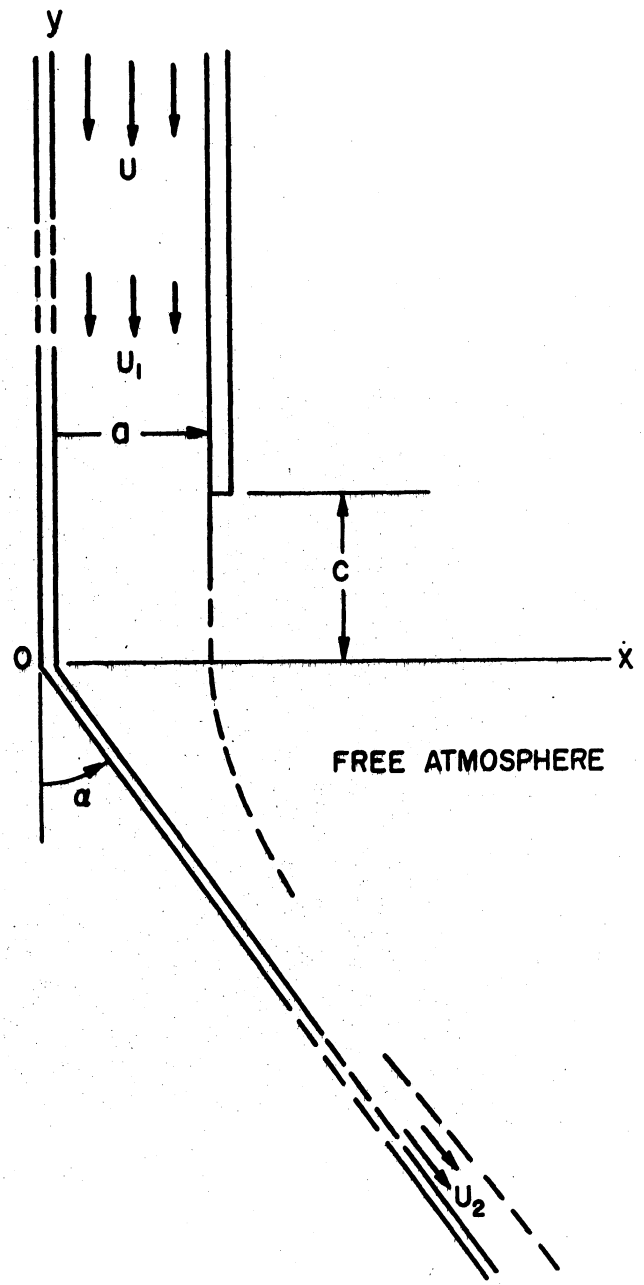

Fig. 16. The theoretical flow of an incompressible, inviscid (ideal) fluid in the case of the efflux from a two-dimensional channel against a semi-infinite plane barrier at an arbitrary angle. With $\alpha = \pi/2$, this flow becomes identical with that in the right- or left-hand half of Fig. 11.

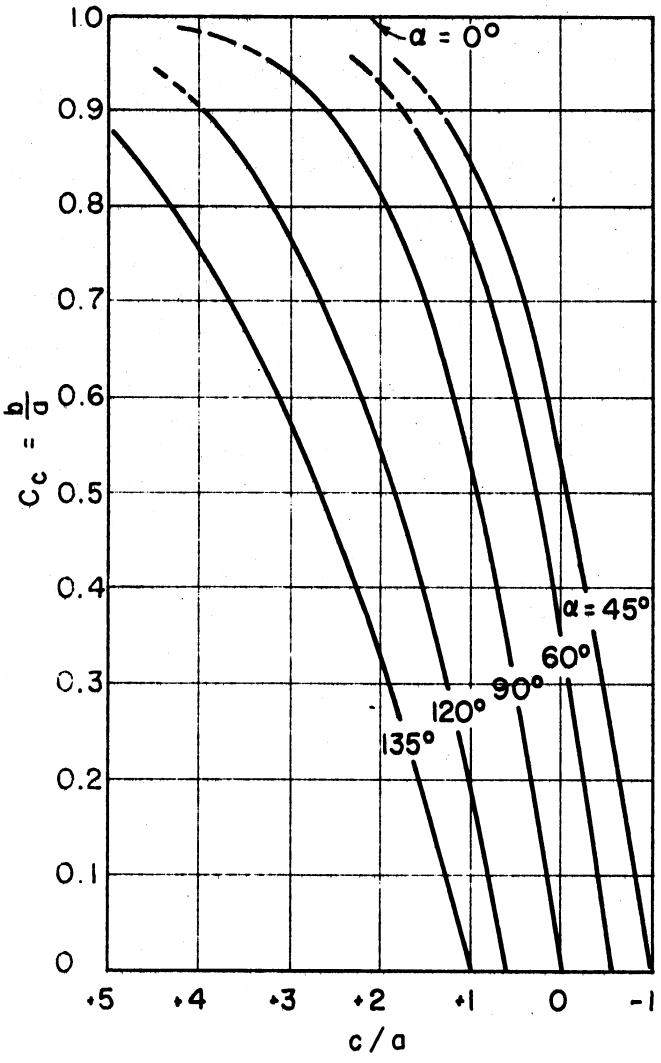

Fig. 17. Coefficient of contraction for the problem of Fig. 16.

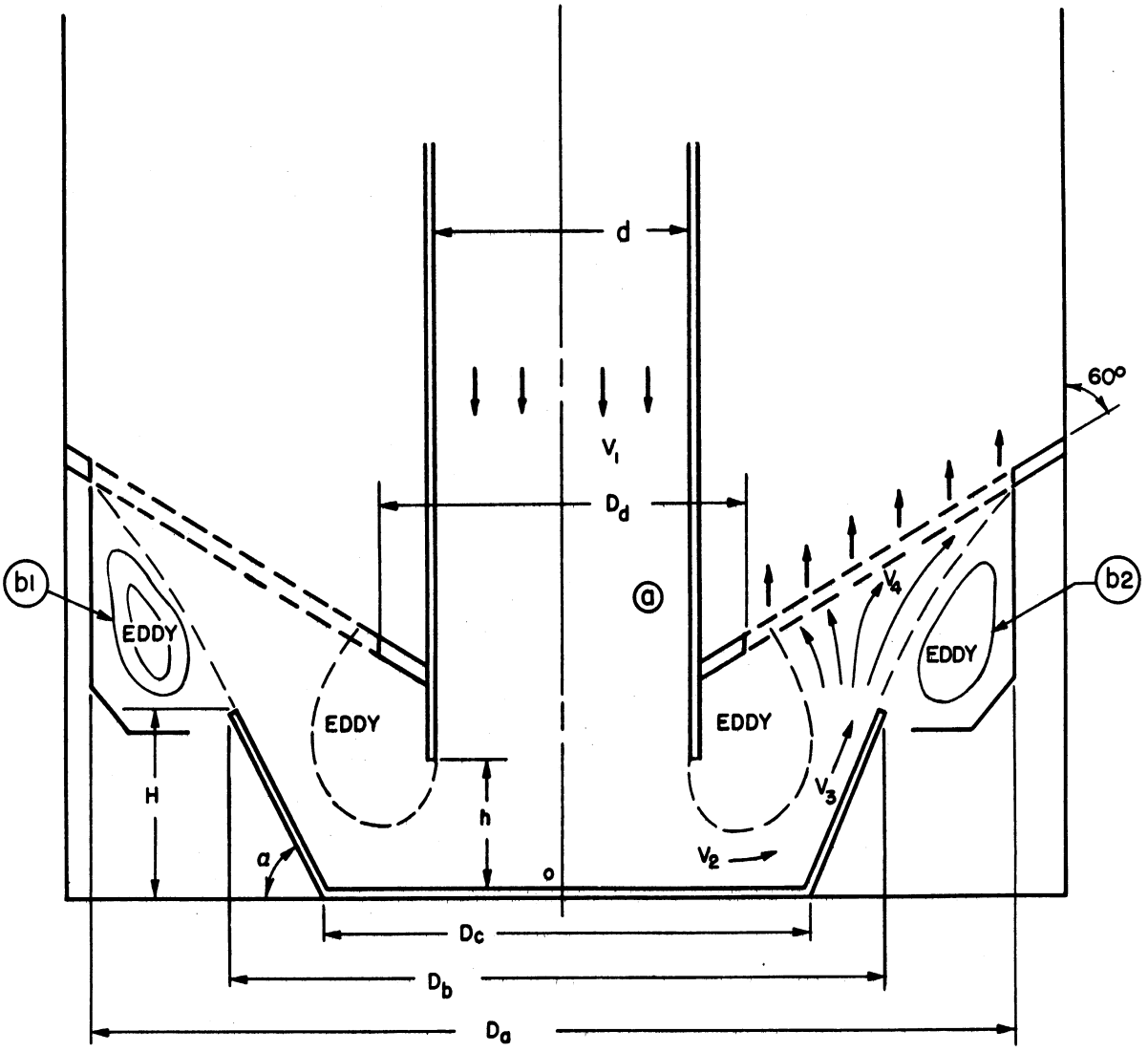

Fig. 18. The character of the actual flow of air through the baffle region of the axially symmetric Donaldson (410 cfm) air cleaner.

Note: Approximately, d = 4.5", h = 1.63", H = 2.5", D_a = 11.188", D_b = 8.0", D_c = 6", D_d = 6.5", α = 68°.

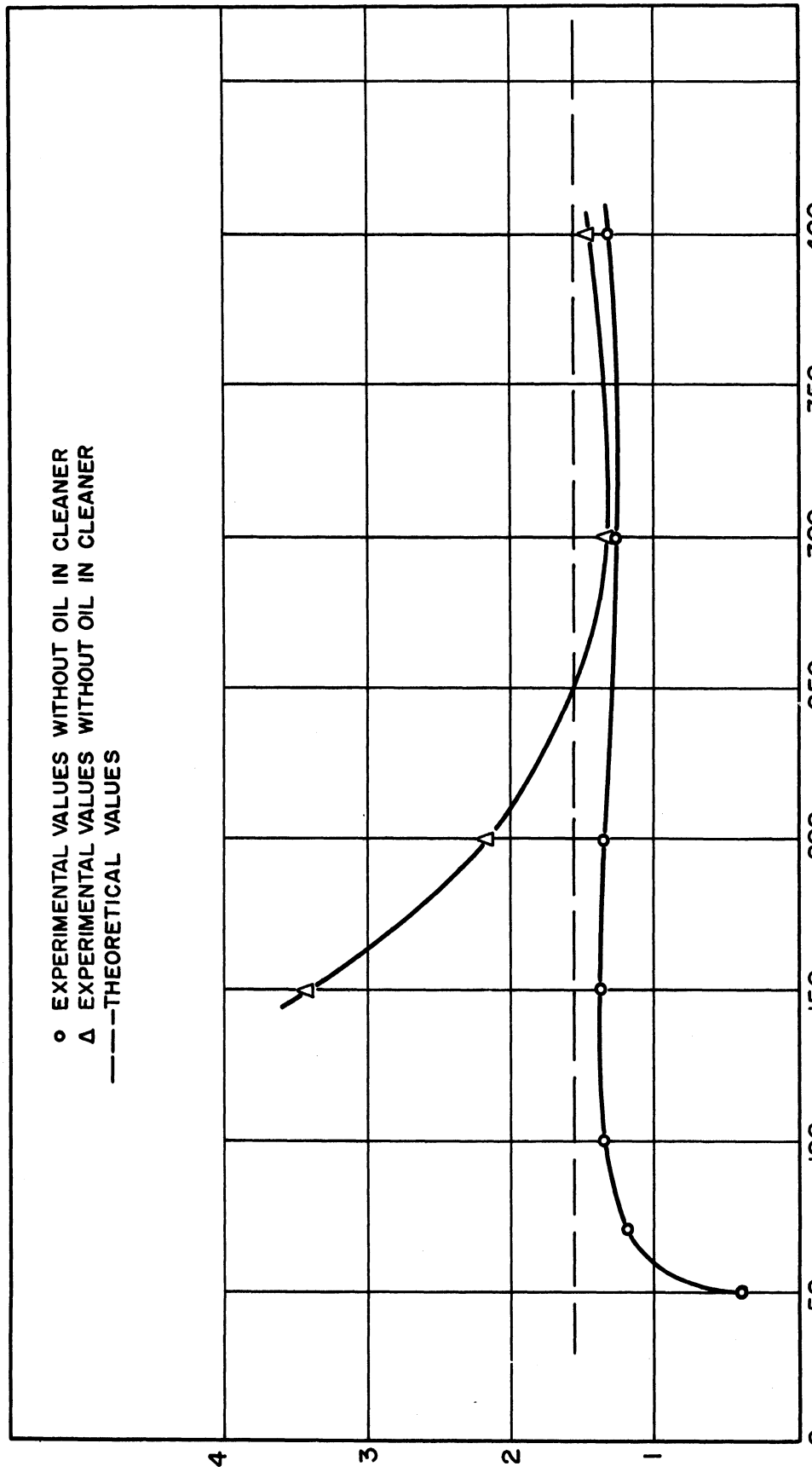

Fig. 19. The pressure drop in the baffle region of the Donaldson 410-cfm air cleaner.

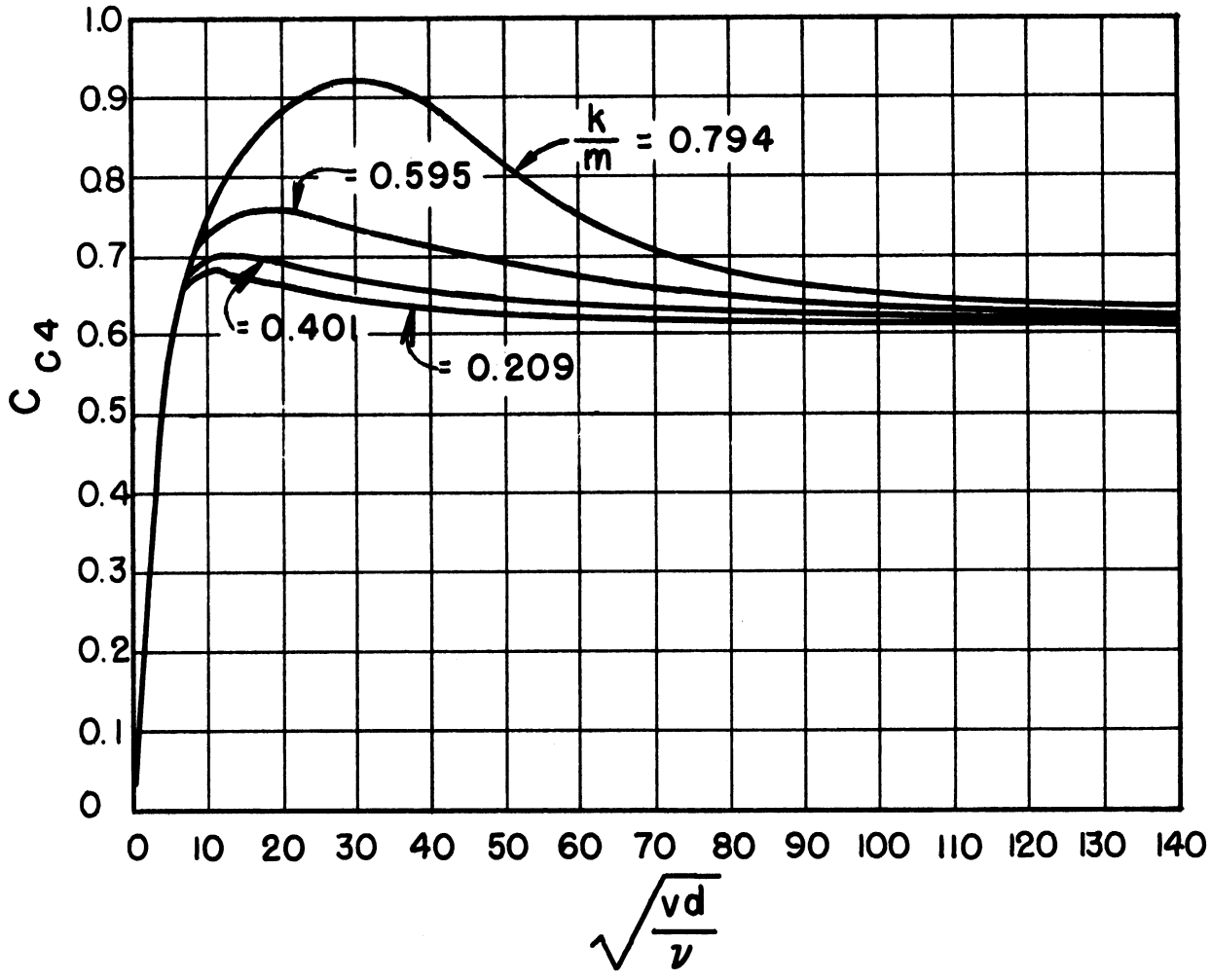

Fig. 20. Discharge coefficients for the plate orifice.

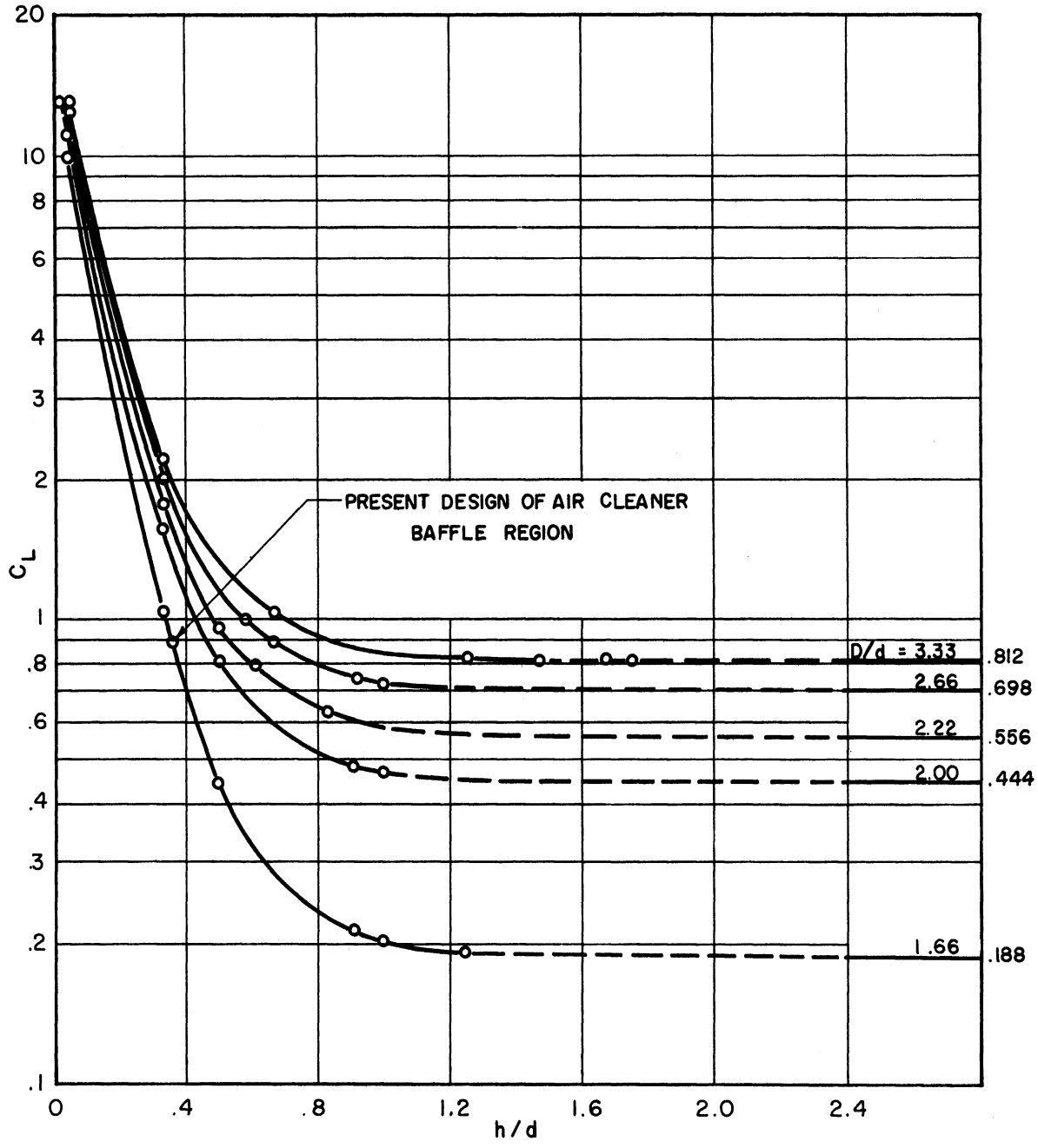

Fig. 21. Theoretical values of C_L for the baffle region of the test apparatus and the air cleaner.

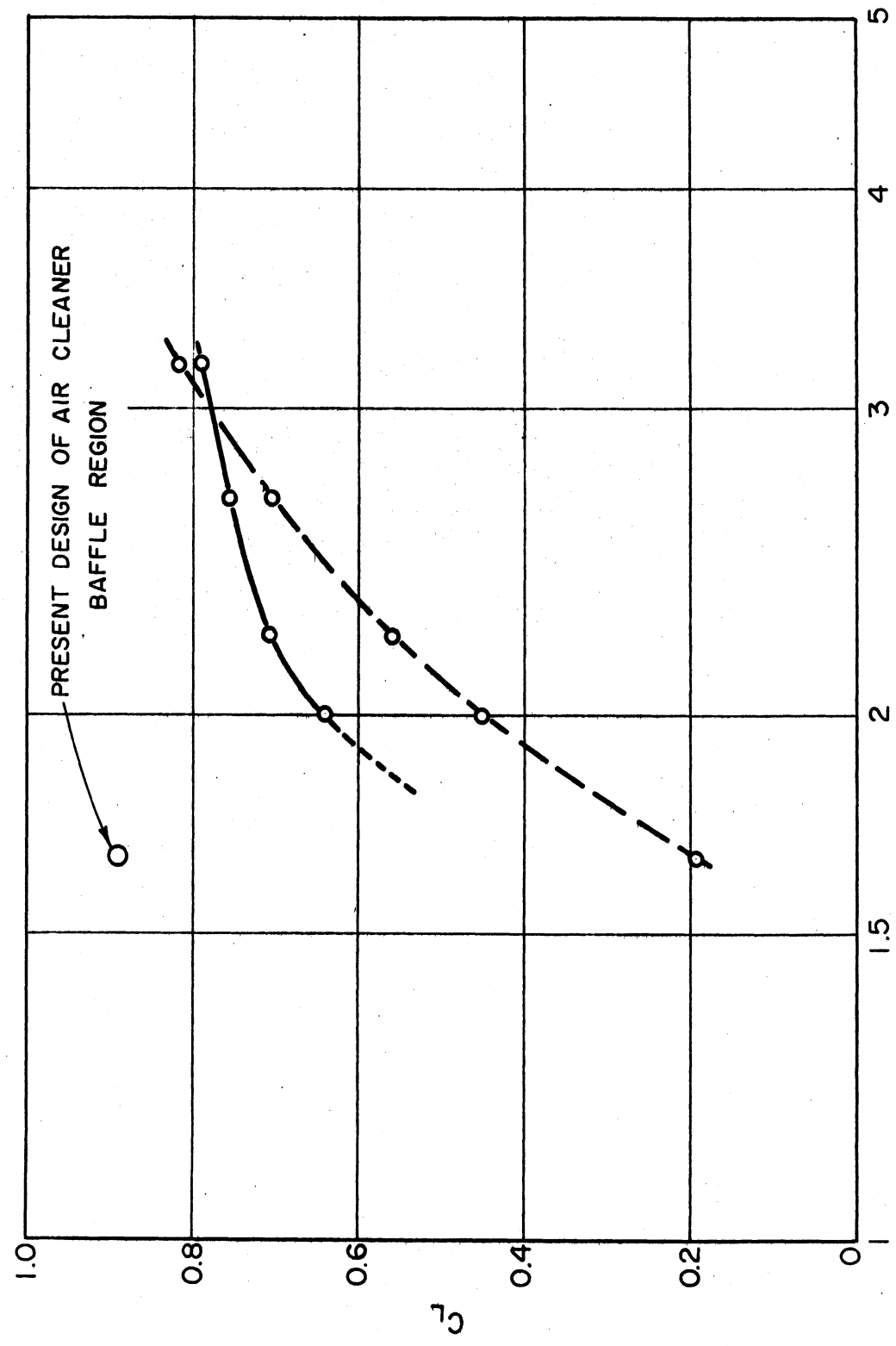

Fig. 22. Minimum values of C_L for the baffle region of the test apparatus and the air cleaner.

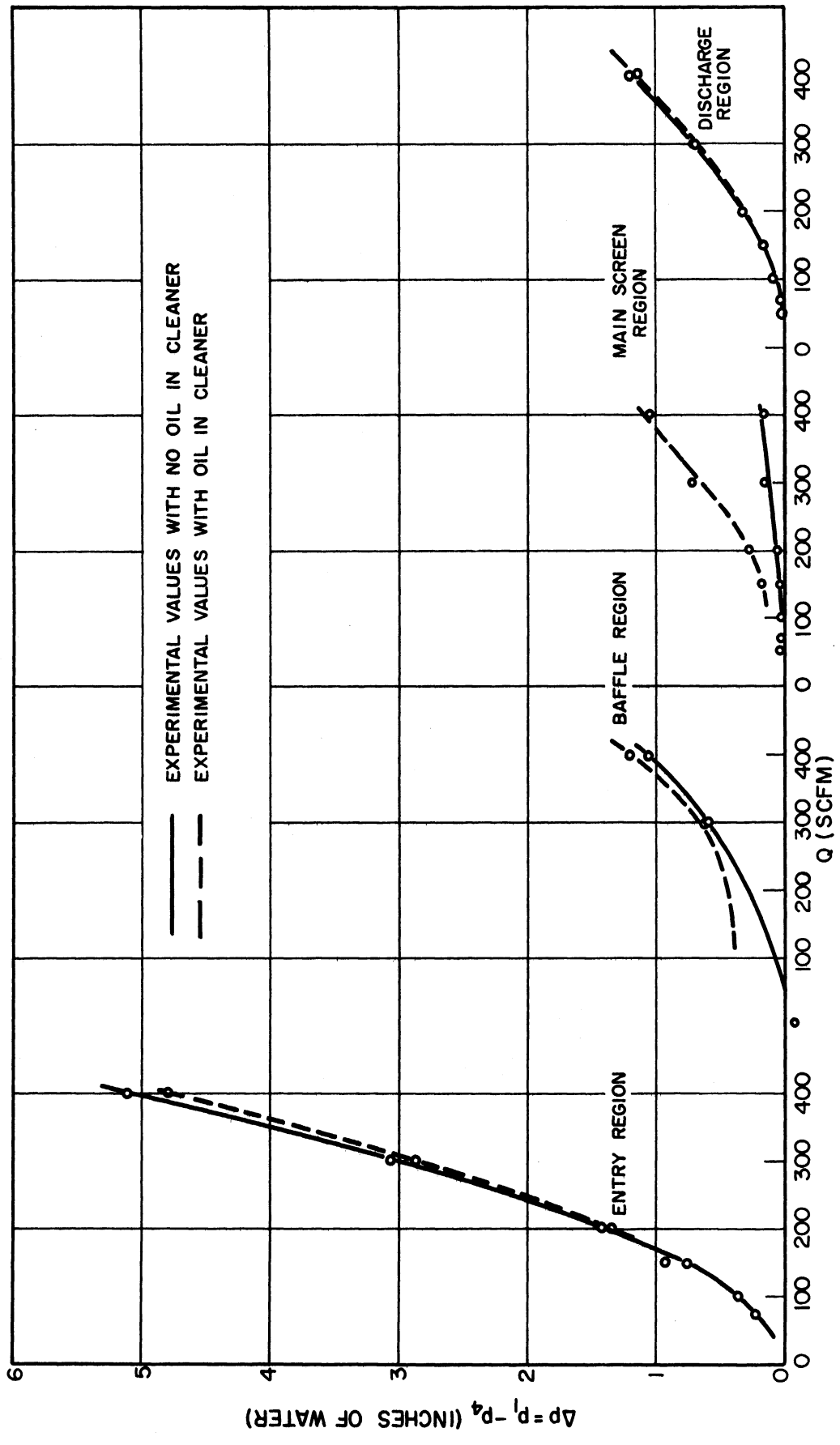

Fig. 23. Average pressure drops in various regions of the air cleaner.

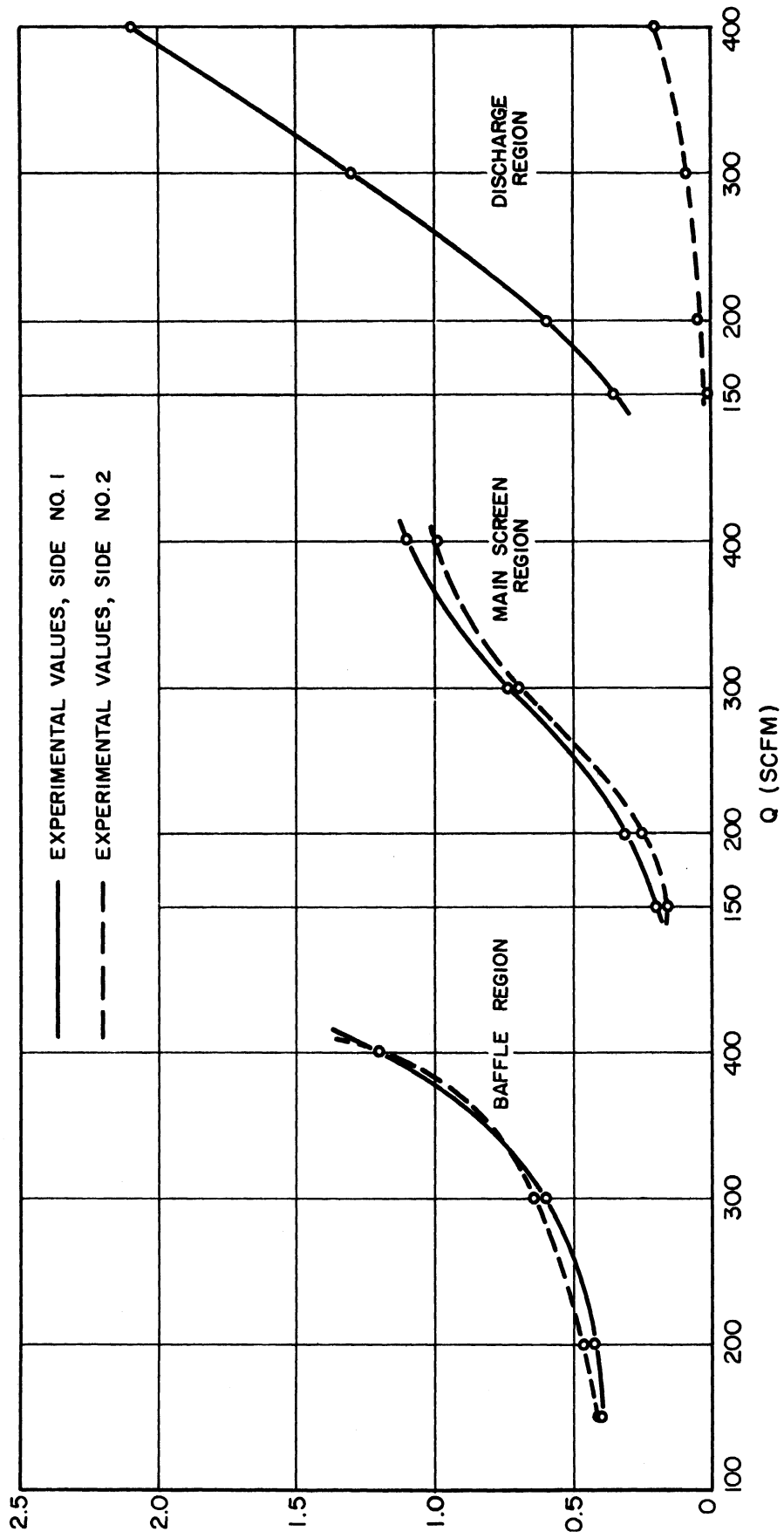

Fig. 24. Circumferential distribution of flow in the air cleaner as indicated by the pressure drop on the outlet side (No. 1) and the opposite side (No. 2) (with oil in cleaner).

CHAPTER III

FLOW STREAMLINES IN AN AIR CLEANER; EFFECTS OF GEOMETRY ON FLOW PATTERN

Introduction

Streamlines were photographed in a two-dimensional model of a Donaldson 410-cfm air cleaner placed in a water channel. The flow was made visible by means of powder on the free surface of the water. The geometry of the model could be varied.

Streamlines were also photographed for the flow of air through the three-dimensional cup-and-tube test apparatus consisting of a vertical down-tube discharging into an upturned cup having a vertical side wall. In this instance, the flow was observed by means of a smoke stream.

The effects of geometry on the flow pattern are most conveniently studied by means of a free-surface flow of water through a two-dimensional model. The validity of the results for qualitative conclusions is discussed and may be seen by a comparison of Figs. 34 and 38, which have the same geometry and represent, respectively, the flow of water through a two-dimensional model and the flow of air through the three-dimensional test apparatus.

The Air Cleaner

It was decided to study first the flow through configurations similar to that of the Donaldson 410-cfm air cleaner. Figure 25 shows one half of a diametral section in the plane containing the discharge opening of the cleaner. For convenience in discussion, Fig. 25 divides the flow path into sections designated as the entry, baffle, main screen, and discharge regions.

Description of the Two-Dimensional Model

Figure 26 is a plan view of the type of model used in the water channel. The geometry could be varied, and Fig. 26 shows that of the Donaldson cleaner. A maximum of two screens was used in the main screen section. In actuality, this region is entirely filled with screen material (Fig. 25). However, the use of one or two screens at particular cross sections was successful in suggesting the principal effects which the screens may have on the flow through them. Due to the use of a water channel, it was necessary to divert the discharge flow through an angle of 180°; therefore, the streamlines downstream from the outlet restriction are not representative of conditions in the air cleaner.

The model was constructed of 1/32-inch-thick brass strips, the edges of which are seen in Fig. 26. As can be seen by comparing Fig. 26 to Fig. 27 or 28, the brass strips appear to be much thicker than 1/32 inch in the photographs, due primarily to parallax and to the refraction of light by the meniscus on the water surface adjacent to the brass strips.

Since it is a two-dimensional representation of a three-dimensional cleaner, the model cannot have true geometrical similarity. However, the latter condition was realized approximately by making the model to a scale of one-third of the actual size of the cleaner as it appears in a diametrical cross section. The lack of true geometric similarity results primarily in the flows at large radii in the air cleaner having relatively lower velocities than those at corresponding points of the model.

When geometrical similarity exists, the model should be tested at water flow rates giving the same range of Reynolds' number as that of the air flow rates encountered in operation of the full-scale air cleaner. Consequently, a direct comparison of the Reynolds' numbers of the model and cleaner has no significance in this case. However, the flow pattern in the baffle section may be expected to vary only slightly with the Reynolds' number. In the screen sections of both the model and cleaner, the velocities are smaller and the flow path is not as definitely dictated by the boundaries. Here the Reynolds' number is a factor and, furthermore, the screens themselves were not reproduced to scale. In this region only limited conclusions may be drawn from the photographs. Nevertheless, the pictures are useful in determining the character of flow entering the screen section and the influence which a change in baffle geometry would have on an existing screen flow.

The use of a free-surface water flow introduces surface tension as a factor not present in the air cleaner. However, its effect may be assumed negligible for present purposes.

Flow in the Entry Region

The flow past the entry baffle and through the central down-tube of the cleaner may be seen along the left hand edge of Fig. 34. In the upper part of the tube, an elongated toroidal eddy near the wall restricts the axial flow. Farther down, the velocity becomes fairly uniform all across the tube. Some of the pressure drop due to the higher velocity of the stream in the eddy section will be regained in the region of uniform flow. However, the net result should be an appreciable loss, due to the diffusion in the expanding flow from the eddy to the point where the velocity becomes uniform across the tube.

This restriction of the flow can be greatly reduced by the addition of a deflector vane to divert a portion of the flow through the region now occupied by the eddy. Preferably, the vane should be designed as a part of a general redesign of the entry region and the hemispherical entry baffle. But if other considerations make it undesirable to change the latter, a vane can be designed as an addition to the present cleaner. This point is discussed more fully in Chapter II.

The General Character of the Flow Through the Baffle and Screen Regions

The photographs of flow through the model, Figs. 27 through 36, will be surveyed briefly before turning attention to details of the baffle and screen regions.

1. Absence of baffle (main stream located near inner wall of main screen section—Figures 27 and 28).

   In the absence of a baffle, the flow adheres to the outer boundaries in the baffle region. It must ultimately deflect inwardly (to the left) in order to leave the screen region. The outer clamping bracket of the first screen determines the location of this deflection (Fig. 27). The stream in the screen region is narrow. The addition of the first screen (Fig. 28) has little effect on the stream, but does introduce an intense and stable eddy below the screen and adjacent to the down-tube.

2. Slanted baffle (main stream located near outer wall of the main screen section—Figs. 29, 30, 31, and 32).

With a slanted baffle (Fig. 29), the stream follows the outer boundaries of both the baffle and screen sections. The addition of the first screen (Fig. 30) does not alter the path of the flow in the screen region, although the stream is wider and of more uniform velocity over its cross section. The flow is quite uniformly distributed across the first screen.

When the first screen becomes plugged near its inner edge (Fig. 31), the stream in the screen region remains wide and uniform. If the screen is plugged near its outer edge (Fig. 32), the stream narnows and flows through the center of the screen section with an eddy region on either side.

3. Slanted baffle (main stream located near inner wall of screen section—Fig. 33).

While the foregoing indicates the outward influence of the slanted baffle on the flow in the screen section, plugging downstream from the first screen may override the action of the baffle. A second screen (Fig. 33) plugged near its outer edge can permanently deflect the stream inwardly even though the slanted baffle is used.

4. Vertical and horizontal baffles (main stream located near inner wall of main screen section—Figs. 34, 35, and 36).

When the baffle is vertical (Fig. 34), the stream is narrow and hugs the outer periphery of the baffle section and the inner periphery of the screen region. The addition of the screen (Fig. 35) does not broaden the stream, which approaches the screen at right angles and remains narrow in the screen region. A comparison of Figs. 28 and 35 indicates that the insertion of a solid boundary (vertical baffle) at the edge of the stream has no effect on the flow path.

A horizontal baffle (Fig. 36) serves to broaden the flow in the screen section, the stream remaining adjacent to the inner boundary.

Control of Flow Pattern in the Baffle and Screen Sections

It is clear that within wide limits the flow in the baffle and screen regions can be made to assume a prescribed pattern. The control can be accomplished by proper design of the baffle region and of the orientation of the first screen, and will be effective as long as the screen region remains unplugged in areas traversed by the main stream. Some specific examples follow.

LOCATION OF MAIN STREAM IN SCREEN REGION

Figures 30 and 36 show fairly wide and uniform streams in the screen region near the outer and inner boundaries, respectively. A different design of the baffle and position of the first screen should permit the flow to approach, to the extent desired, a uniform distribution across the entire screen section. Presumably, the most desirable flow pattern in the screen section is partially determined by any return oil flow which is intended to occur. It is clear that the eddy region bounding the main stream may be located at either the inner or the outer boundary as desired. New designs can be worked out through the use of the channel.

FLOW ALONG THE BAFFLE

Figures 29 through 36 indicate that a curved baffle would direct a more effective jet at the first screen. Such a baffle may also reduce the pressure loss in this region and, if desirable, assist in maintaining the eddy under the outer part of the first screen.

OUTER EDDY IN THE BAFFLE REGION

Figures 30, 31, 32, and 33 have the baffle configuration of the Donaldson cleaner. The outer (right hand) portion of the space immediately below the first screen is occupied by an eddy rotating clockwise. In Fig. 32 where the outer part of the first screen was plugged, this eddy was very stable over a range of flow rates and entirely filled the outer portion of the space below the screen. Under the conditions of Figs. 30, 31, and 33, the eddy was erratic and at some flow rates did not extend down to the partition immediately below it. At such times, the fluid just above this partition was either oscillating or rotating slowly in a counter-clockwise sense.

PLUGGING OF THE SCREENS

Unavoidable loading of portions of the screens during operation may cause the flow in the main screen region to deviate significantly from any desired pattern achieved at the outset. If this condition unduly curtails the period of effective operation of the cleaner, the cleaner should be redesigned so that unavoidable loading is more uniformly distributed throughout the screen region. A need for more uniform flow in the screen of the discharge region is shown in Chapter II. Some remedies are suggested there.

Air Flow Streamlines in the Cup-and-Tube Test Apparatus

The air flow in this apparatus was studied by introducing smoke at the bottom of the upturned cup. Specifically, smoke was inserted at a point where the air had left the down-tube and was flowing radially outward parallel to the bottom of the cup. The apparatus and the air flow were symmetrical about the vertical axis of the down-tube. The flow boundaries formed by the down-tube and cup are indistinct in the photographs obtained. Consequently, a drawing (Fig. 37) is included which shows the portion of the apparatus in which the flow was photographed.

Figure 38 is a photograph of the flow through the cup and upward along the outer surface of the down-tube. The outlet of the smoke supply tube can be seen at the bottom of the cup. The approximately elliptical region just above the smoke tube outlet was the location of a stable eddy which appears as a dark region since it contained very little smoke. At greater air flows this eddy became elongated and extended higher up the outer surface of the down-tube. As in the analogous two-dimensional case (Fig. 34), Fig. 38 clearly shows that, after passing the stationary eddy, the jet is diverted radially inward and flows along the surface of the down-tube. Higher up the tube, the air stream broadens gradually.

The dark region above the cup and to the left of the main stream is the location of a large, slowly rotating eddy similar to those already seen in the two-dimensional cases. Figures 39 and 40 show the beginning of a small eddy of a type generated at intervals on the boundary between the jet and the large boundary eddy. Such eddies were then drawn upward by the stream, as indicated by Fig. 38, where an eddy can be seen at the top of the photograph. This unsteady condition at the edge of the stream was predominant at lower flows under which circumstances fluctuations in the total flow rate were observed. A similar behavior was noted occasionally in the water channel. In the air cleaner, it is expected that the distributed screens will suppress this effect.

Flow Around the Lower End of the Down-Tube

The stationary eddy observed above the smoke tube outlet (Fig. 38) was decidedly present in the corresponding part of the two-dimensional model where it appeared just below the inner (left hand) end of the first screen. However, it is not clearly shown in the photographs (Figs. 29 through 36) because in some instances (Fig. 34, especially) the film exposure was too short

for this purpose, and in other cases the meniscus and parallax caused an apparent broadening of the nearby boundary and obscured part of the eddy.

By placing a rounded obstruction on the inner surface of the down-tube just above its lower end, the stationary eddy was nearly eliminated in the two-dimensional model. This obstruction is indicated by a dotted line in Fig. 26. The elimination of this eddy should assist in obtaining a wide uniform stream in the screen region and may reduce the pressure loss somewhat. Such a change produces a more uniform flow in the baffle region, but reduces the velocity of the fluid leaving the cup, especially at the upper end of the slanted baffle.

Pressure Loss in the Air Cleaner

Suggestions have been made in foregoing sections for reducing the pressure loss in the air cleaner, particularly at the upper and lower ends of the down-tube. However, such reductions may be negligible compared to the necessary loss in the screen or other regions. In order to investigate this phase of the problem, measurements were made of the pressure loss in each of the regions of the cleaner. This work is described in Chapter II and, together with the results of the present chapter, leads to several conclusions regarding air-cleaner design.

Summary and Conclusions

While some important conclusions have been reached, it may be desirable to obtain additional flow pictures. The present method for photographing the flow was worked out only recently, and the experience gained has suggested improvements in the technique which should result in more readily interpreted photographs.

The flow pictures indicate that the air flow in the cleaner can be studied in the water channel and can be controlled through the design geometry. It appears that the flow in the screen region is nonuniform and that a curved baffle and an obstruction of the bottom of the down-tube may improve this condition. A vane below the entry baffle should reduce the pressure drop considerably. A full appraisal of these changes requires measurements of the pressure drop in the various regions of the air cleaner. Such data are analyzed in the earlier chapter on pressure drop and pressure loss in the air cleaner.

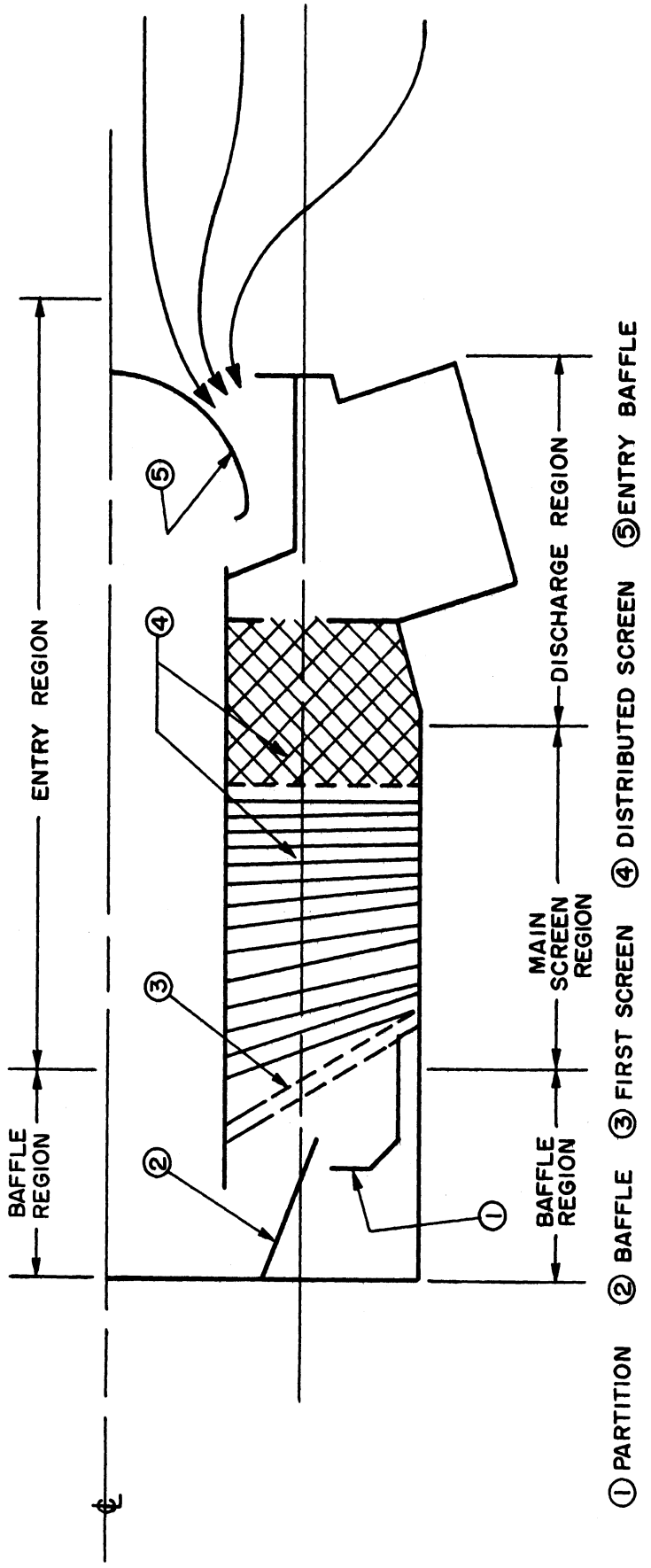

Fig. 25. Half section through Donaldson 410-cfm air cleaner.

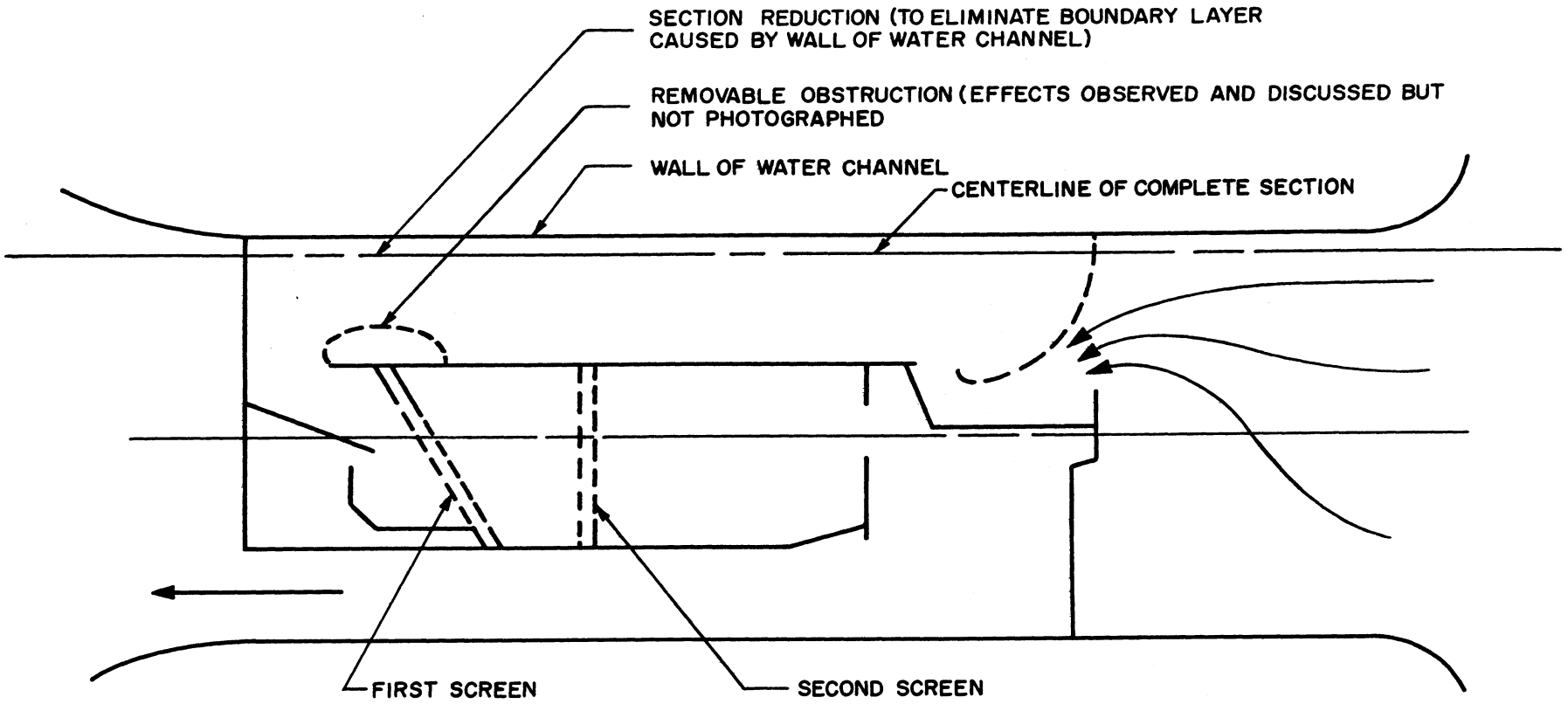

Fig. 26. Plan view of two-dimensional model of Donaldson 410-cfm air cleaner, representing one half of a diametral section of the air cleaner.

Note: See Fig. 1 for other names of components. Dashed lines indicate components removable in the model. The baffle and partition were removable in a second similar model.

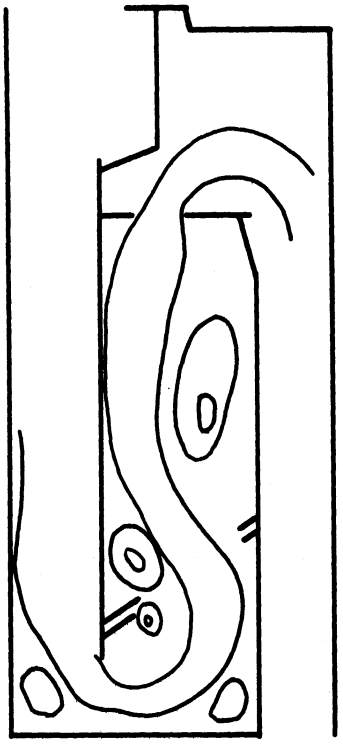

Fig. 27.

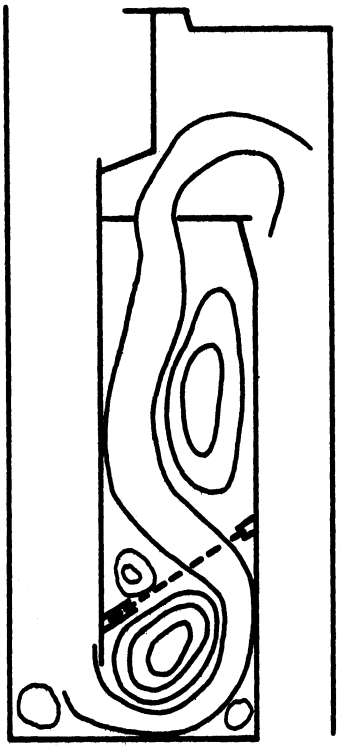

Fig. 28.

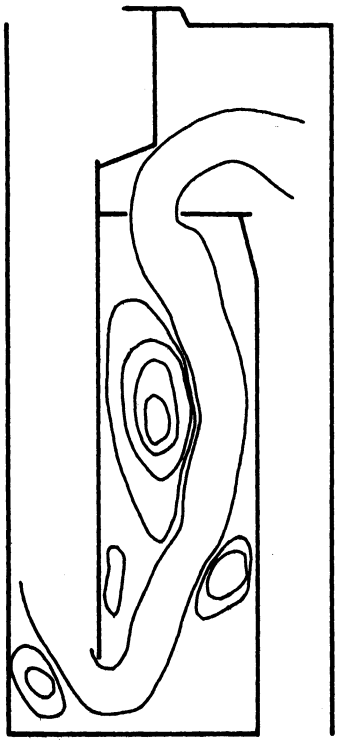

Fig. 29.

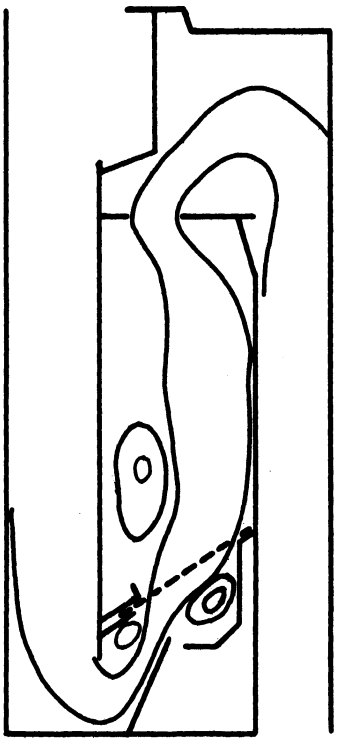

Fig. 30.

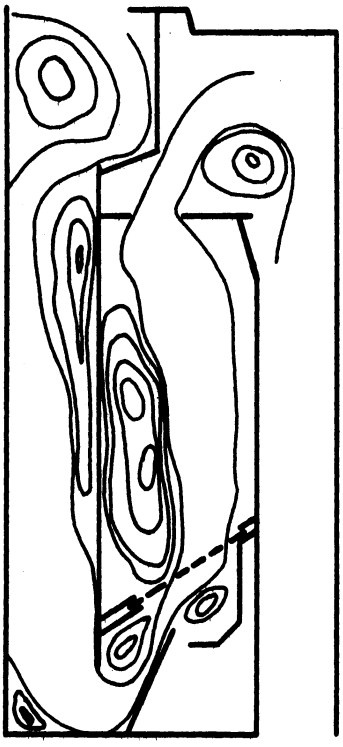

Fig. 31.

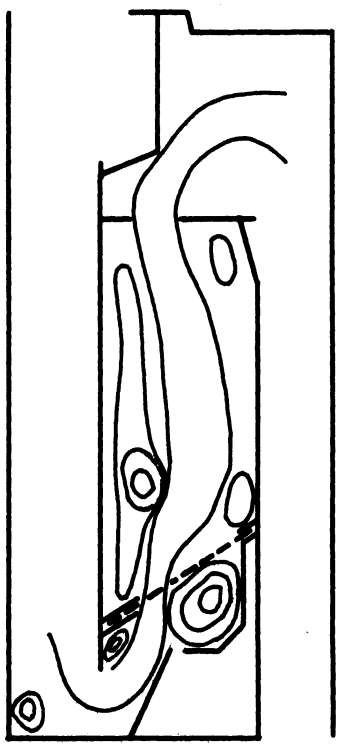

Fig. 32.

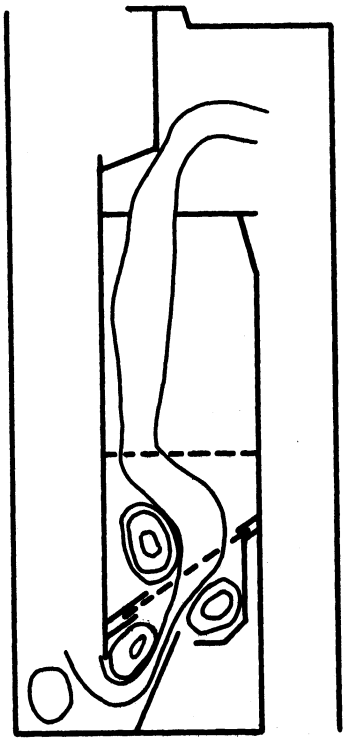

Fig. 33.

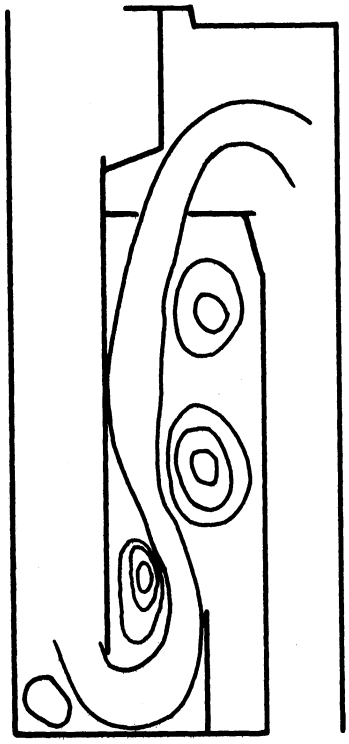

Fig. 34.

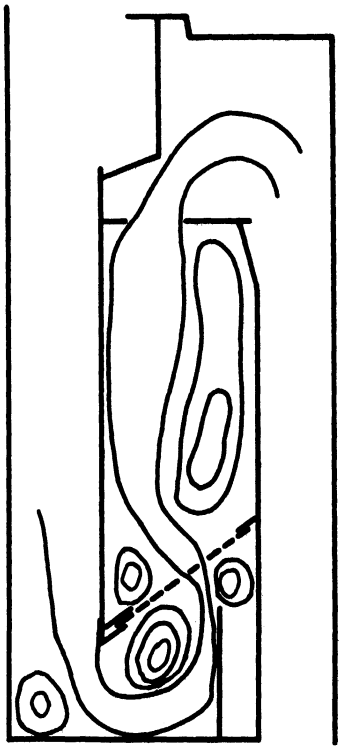

Fig. 35.

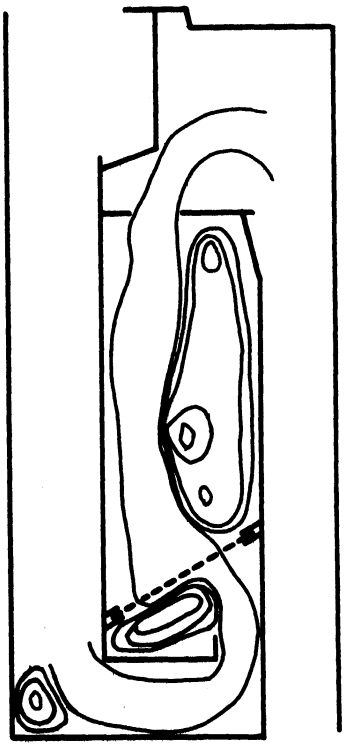

Fig. 36.

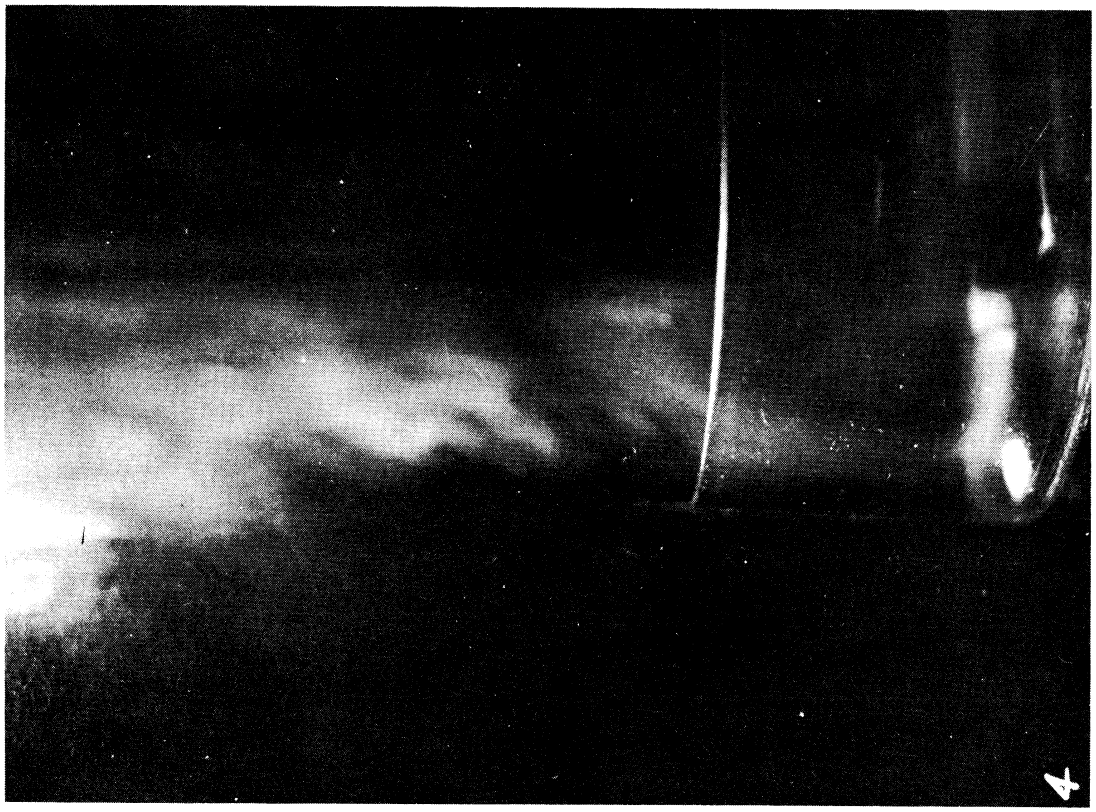

Fig. 38. Flow pattern.

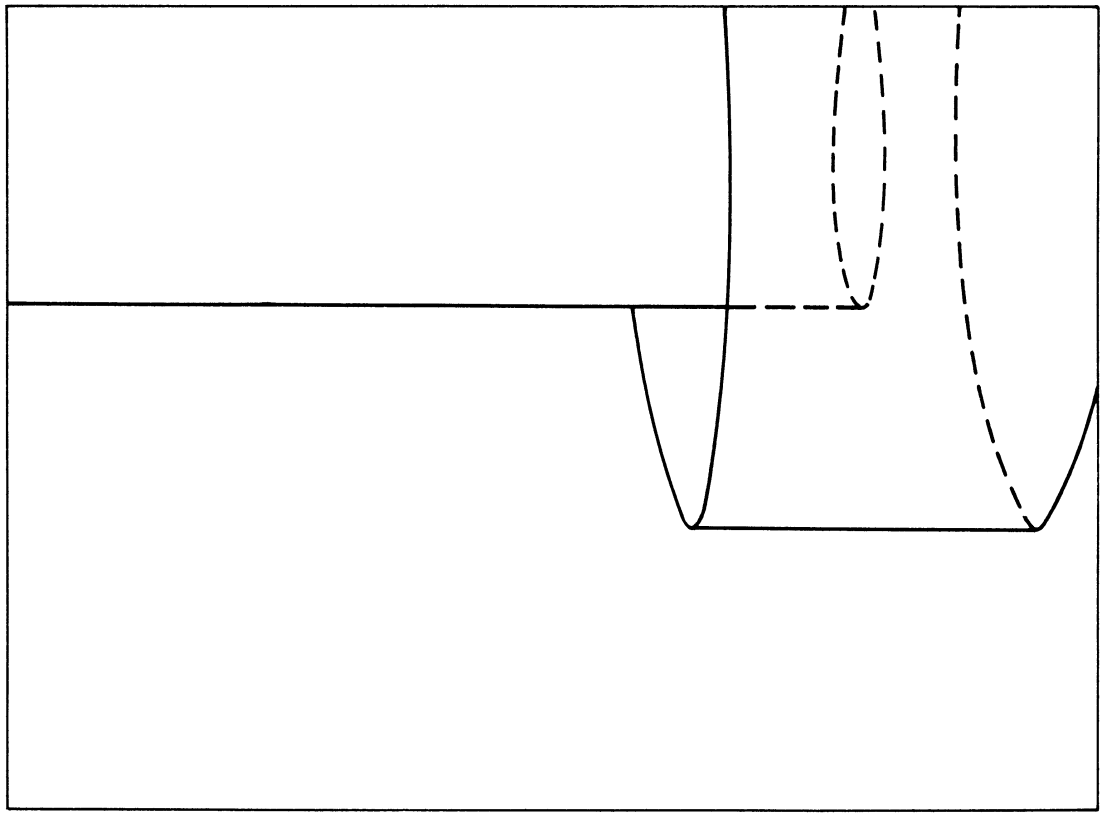

Fig. 37. Flow pattern.

Fig. 40. Flow pattern.

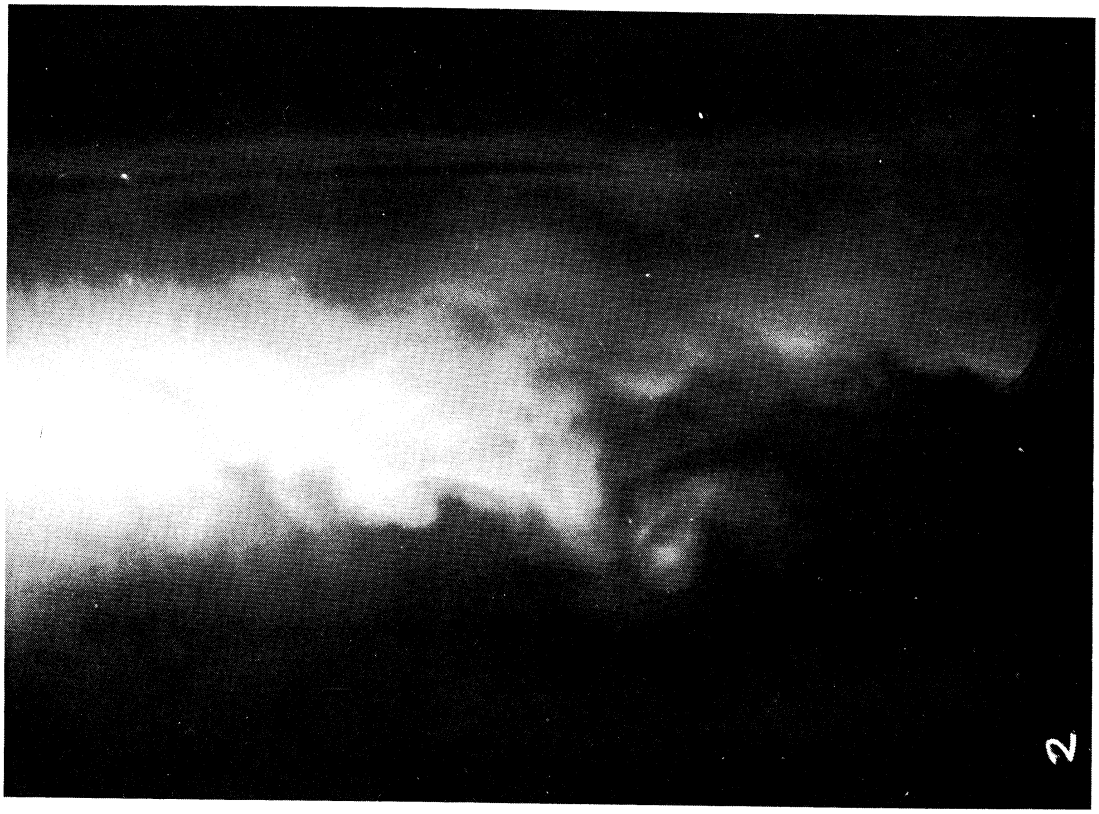

Fig. 39. Flow pattern.